ESCOLA SUPERIOR DE TECNOLOGIA DA SAÚDE DO PORTO
INSTITUTO POLITÉCNICO DO PORTO

Ana Cláudia dos Santos Pereira

EFFECT OF OXIDATIVE STRESS UPON ABSORPTION OF GLUCOSE BY THE HUMAN PLACENTA

IN VITRO STUDIES WITH BEWO CELLS

Dissertação submetida à Escola Superior de Tecnologia a Saúde do Porto para cumprimento dos requisitos necessários à obtenção do grau de Mestre em Tecnologia Bioquímica em Saúde, realizada sob a orientação científica de Professora Doutora Fátima Martel, Professora Associada do Departamento de Bioquímica da Faculdade de Medicina do Porto e Professora Doutora Cristina Prudêncio, Coordenadora da Área Técnico-Científica do Departamento das Ciências Químicas e das Biomoléculas da Escola Superior de Tecnologia da Saúde do Porto, Instituto Politécnico do Porto e sob a co-orientação da Professora Doutora Elisa Keating, Professora Auxiliar do Departamento de Bioquímica da Faculdade de Medicina do Porto.

September, 2012

Acknowledgments

À Escola Superior de Tecnologia da Saúde do Porto, em especial a Área Científica das Ciências Químicas e das Biomoléculas, pelo acolhimento.

À Faculdade de Medicina da Universidade do Porto e ao Departamento de Bioquímica, por me terem acolhido e apoiado na execução deste projecto.

À Professora Doutora Fátima Martel, por toda a disponibilidade, simpatia, transmissão de conhecimentos e orientação científica, apesar da preenchida agenda, um sincero obrigado.

À Professora Doutora Cristina Prudêncio, o meu agradecimento pelo apoio e incentivo, pela simpatia e transmissão de conhecimentos.

Ao Professor Doutor Rúben Fernandes, por toda a disponibilidade, apoio, compreensão, amizade e orientação ao longo de todo o curso de mestrado, um sincero obrigado.

Aos meus colegas de laboratório e à Professora Doutora Elisa Keating, no Departamento de Bioquímica da Faculdade de Medicina da Universidade do Porto, o meu agradecimento por todo o apoio científico e laboratorial e por toda a ajuda, companheirismo e simpatia, sem os quais não teria sido possível a concretização deste projecto.

Aos meus colegas de trabalho na Escola Superior de Tecnologia da Saúde do Porto, por todo o companheirismo ao longo do mestrado, bem como pelo espírito de alegria e boa disposição e, em particular, ao César Pimenta, por toda a ajuda, apoio e amizade.

Ao Prof. J.T.Guimarães e Patologia do CHSJ, pela disponibilidade e prontidão, cuja colaboração foi sem dúvida uma mais-valia para a execução do projecto.

Um profundo e sincero agradecimento a todos os meus Amigos, pela compreensão e constante apoio, sem os quais teria sido impossível manter-me optimista e revitalizada.

E porque os últimos são os primeiros, um sincero agradecimento à minha família, em particular à minha mãe, por todo o apoio incondicional, tão importante não só no meu percurso académico mas também na minha formação pessoal.

1 Index

2 Tabels índex

3 Figures índex

4 Abreviations

ROS	Reactive Oxygen Species
^{3}H-DG	^{3}H-2-deoxy-D-glucose
tBOOH	*tert*butylhydroperoxide
SGLT	sodium-glucose linked transporter
GLUT	glucose facilitative transporters
GSx	Total Glutathione
GSH	Reduced Glutathione
GSSG	Oxidized Glutathione
K_{in}	constant for inward transport
K_{out}	constant for outward transport
A_{max}	maximum acumulation
qRT-PCR	quantitative reverse transcription real-time-PCR
mRNA	messenger ribonucleic acid
LDH	enzyme lactate dehydrogenase
SRB	sulforhodamine B
TBARS	thiobarbituric acid reactive substances
TEER	transepithelial resistance
P_{app}	apparent permeability
cyt B	cytochalasin B
phlor	phloretin
PI3K / Akt	phosphatidylinositol 3-kinases
PKC	protein kinase C
Vit E	Vitamine E
NAC	N-acetylcysteine
Resv	resveratrol
Querc	quercetin
EGCG	epigallocatechin-3-gallate

5 Abstract

Pregnancy is a dynamic state and the placenta is a temporary organ that, among other important functions, plays a crucial role in the transport of nutrients and metabolites between the mother and the fetus, which is essential for a successful pregnancy.

Among these nutrients, glucose is considered a primary source of energy and, therefore, fundamental to insure proper fetus development. Several studies have shown that glucose uptake is dependent on several morphological and biochemical placental conditions.

Oxidative stress results from the unbalance between reactive oxygen species (ROS) and antioxidants, in favor of the first. During pregnancy, ROS, and therefore oxidative stress, increase, due to increased tissue oxygenation. Moreover, the relation between ROS and some pathological conditions during pregnancy has been well established.

For these reasons, it becomes essential to understand if oxidative stress can compromise the uptake of glucose by the placenta.

To make this study possible, a trophoblastic cell line, the BeWo cell line, was used. Experiments regarding glucose uptake, either under normal or oxidative stress conditions, were conducted using *tert*-butylhydroperoxide (tBOOH) as an oxidative stress inducer, and ^{3}H-2-deoxy-D-glucose (^{3}H-DG) as a glucose analogue. Afterwards, studies regarding the involvement of glucose facilitative transporters (GLUT) and the phosphatidylinositol 3-kinases (PI3K) and protein kinase C (PKC) pathways were conducted, also under normal and oxidative stress conditions. A few antioxidants, endogenous and from diet, were also tested in order to study their possible reversible effect of the oxidative effect of tBOOH upon apical ^{3}H-DG uptake. Finally, transepithelial studies gave interesting insights regarding the apical-to-basolateral transport of ^{3}H-DG.

Results showed that ^{3}H-DG uptake, in BeWo cells, is roughly 50% GLUT-mediated and that tBOOH (100 μM; 24h) decreases apical ^{3}H-DG uptake in BeWo cells by about 33%, by reducing both GLUT- (by 28%) and non-GLUT-mediated (by 40%) ^{3}H-DG uptake. Uptake of ^{3}H-DG and the effect of tBOOH upon ^{3}H-DG uptake are not dependent on PKC and PI3K. Moreover, the effect of tBOOH is not associated with a reduction in GLUT1 mRNA levels. Resveratrol, quercetin and epigallocatechin-3-gallate, at 50 μM, reversed, by at least 45%, the effect of tBOOH upon ^{3}H-DG uptake. Transwell studies show that the apical-to-basolateral transepithelial transport of ^{3}H-DG is increased by tBOOH.

In conclusion, our results show that tBOOH caused a marked decrease in both GLUT and non-GLUT-mediated apical uptake of ^{3}H-DG by BeWo cells. Given the association of increased oxidative stress levels with several important pregnancy pathologies, and the important role of glucose for fetal development, the results of this study appear very interesting.

6 Key-words

Placenta, BeWo, Oxidative Stress, Glucose Absorption

7 Resumo

A gravidez é um estado dinâmico e a placenta o órgão temporário que, entre diversas e importantes funções, apresenta o papel fundamental de ser responsável pela troca de nutrientes, e metabolitos, entre a mãe e o feto, essenciais para uma gravidez bem-sucedida.

Dentro da classe dos nutrientes, a glicose apresenta-se como a fonte primordial de energia para o feto, sendo portanto imprescindível para o correto desenvolvimento deste. Vários estudos demostram que a absorção de glicose, ao nível da placenta, está dependente de diversas condições morfológicas e bioquímicas.

O stresse oxidativo resulta de um desequilíbrio entre as espécies reactivas de oxigénio (ROS: *reactive oxygen species*) e antioxidantes, em favorecimento dos primeiros. Durante a gravidez, estas espécies, e portanto o stresse oxidativo, aumentam devido ao aumento da oxigenação dos tecidos placentários. Adicionalmente, a relação entre ROS e diversas patologias na gravidez já foi bem estabelecida.

Por estas razões, torna-se essencial compreender se o stresse oxidativo poderá comprometer a absorção da glicose ao nível da placenta.

Para tal, uma linha celular, as células BeWo, foi usada. Experiências relacionadas com a absorção de glicose, sob condições normais e de stresse oxidativo foram feitas usando o *tert*–butilhidroperóxido (tBOOH) como indutor de stresse e um análogo radioactivo da glicose, a ^{3}H-2-desoxi-D-glicose (^{3}H-DG). Posteriormente, estudos sobre o papel dos transportadores facilitativos de glicose (GLUT) e de algumas vias de sinalização, phosphatidilinositol 3-cinases (PI3K) and proteína cinase C (PKC), na absorção da ^{3}H-DG, em condições normais e de stresse oxidativo, bem como o potencial efeito de reversão de alguns antioxidantes, endógenos e da dieta, foram feitos. Finalmente, foram ainda realizados estudos sobre o papel do stresse oxidativo no transporte transepitelial, no sentido apical-basolateral, de ^{3}H-DG.

Os resultados obtidos mostram que aproximadamente 50% do transporte da ^{3}H-DG nas células BeWo é mediado pelo GLUT e que o tBOOH (100 μM; 24h) reduz essa absorção em cerca de 33%, reduzindo quer a captação mediada pelo GLUT (em 28%) quer a captação não mediada pelo GLUT (em 40%). A captação de ^{3}H-DG e o efeito do tBOOH nessa mesma captação não são dependentes nem da PKC nem da PI3K. . Adicionalmente, o efeito do tBOOH não está associado a uma redução nos níveis de RNAm do GLUT1. O resveratrol, a quercetina e epigalocatequina-3-galato, 50 μM, reverteram, em pelo menos 45%, o efeito do tBOOH na

captação de ^{3}H-DG. Estudos em *Transwells* mostram que o transporte transepitelial de ^{3}H-DG, no sentido apical-basolateral, aumenta em resposta ao tBOOH.

Em conclusão, este estudo mostra que o tBOOH causa uma redução marcada na captação de ^{3}H-DG, quer mediada pelo GLUT, quer não mediada pelo GLUT, em células BeWo. Sabendo que um aumento nos níveis de stresse oxidativo está associado a numerosas patologias da gravidez, e que a glicose é um nutriente essencial para o feto, os resultados deste estudo parecem-nos de facto importantes.

8 Palavras-chave

Placenta, BeWo, Stresse Oxidativo, Captação de Glicose

9.1 The placenta and the fetus

Pregnancy is a dynamic state that begins with an important stage, the embryogenesis, where an ovum is fertilized and then undergoes a continuous process involving successive mitosis, reaching an undifferentiated state called morula. The morula travels to the uterus, where it begins absorpting uterine fluid, forming a central cavity. At this point it is known as blastocyst. The blastocyst consists of a peripheral layer – the trophoblast – and a central lumen, known as inner cell mass or blastocyst cavity (Fig. 1).

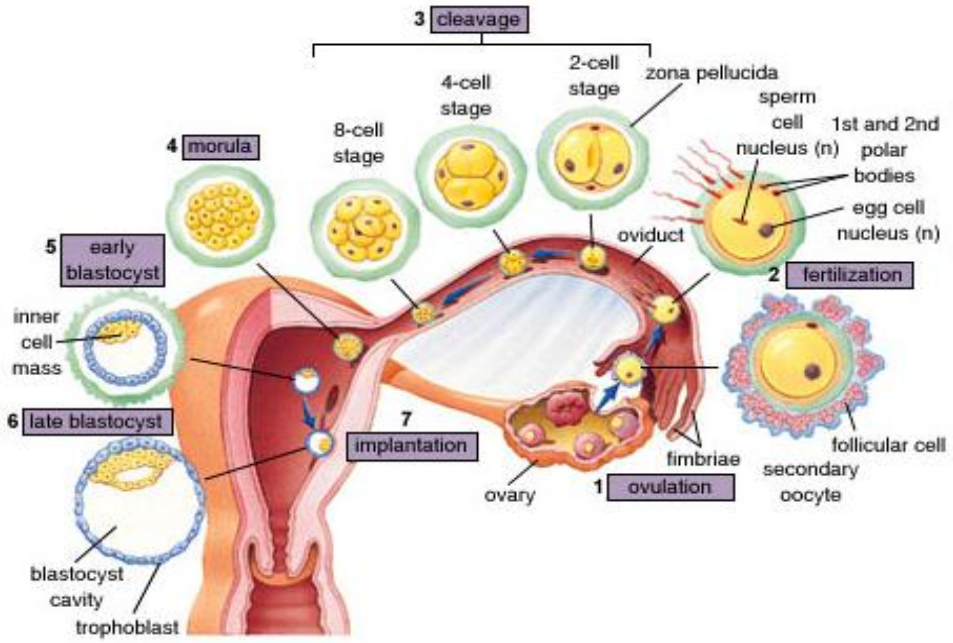

Figure 1: The several phases of the embryo in the first week of gestation [3].

It then undergoes other important stages, namely implantation, placenta formation and organogenesis [4, 5].

Along with the maternal contribution, it is from the trophoblast that the placenta arises, while the embryo develops from the inner cell mass. The trophoblast develops into two layers: an inner layer called cytotrophoblast, which remains as a single layer of cells, and an outer layer, called syncytiotrophoblast cells, resulting from the fusion of cytotrophoblast cells to form a continuous multinucleated syncytium that becomes increasingly broad and develops finger-like projections into the endometrium. There is also a third layer, the intermediate trophoblast, that, like the name suggests, is found between the two previously mentioned layers, and which has an importance role in invading the endometrium [4].

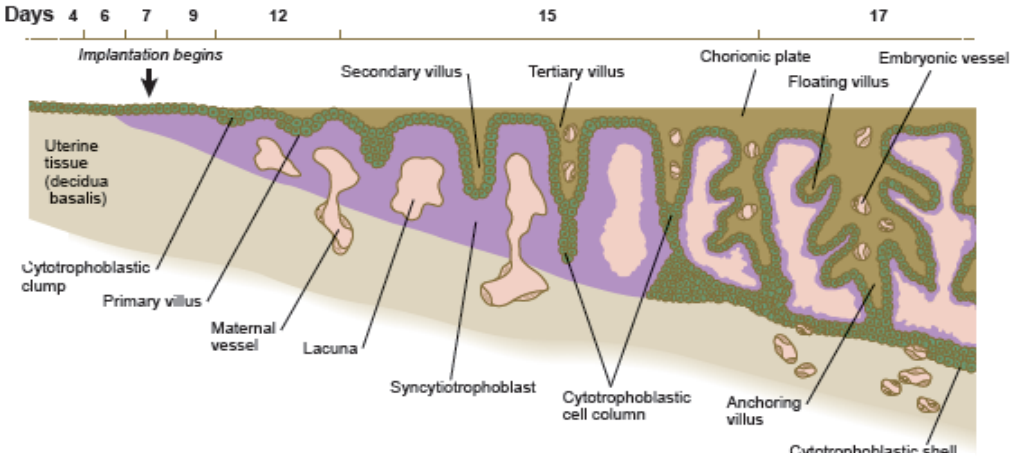

Figure 2: Stages in the formation of a chorionic villus, starting with a cytotrophoblastic clump at the far left and progressing over time to an anchoring villus at right [(4)].

The basal membrane of the cytotrophoblast, which lacks microvilli projections, becomes the basal membrane of the placenta, facing the fetal circulation, while the apical side of the syncytiotrophoblast becomes the apical membrane of the placenta, a microvillous brush border membrane that constitutes the mother-facing plasma membrane (Fig. 2) [(6)]. Invasion of the intermediate trophoblast causes endometrial capillaries leakage resulting in the invasion of maternal blood into the lacunae, a network of spaces that will subsequentially allow the exchange of substances between the mother and the fetus (Fig. 3) [(4)].

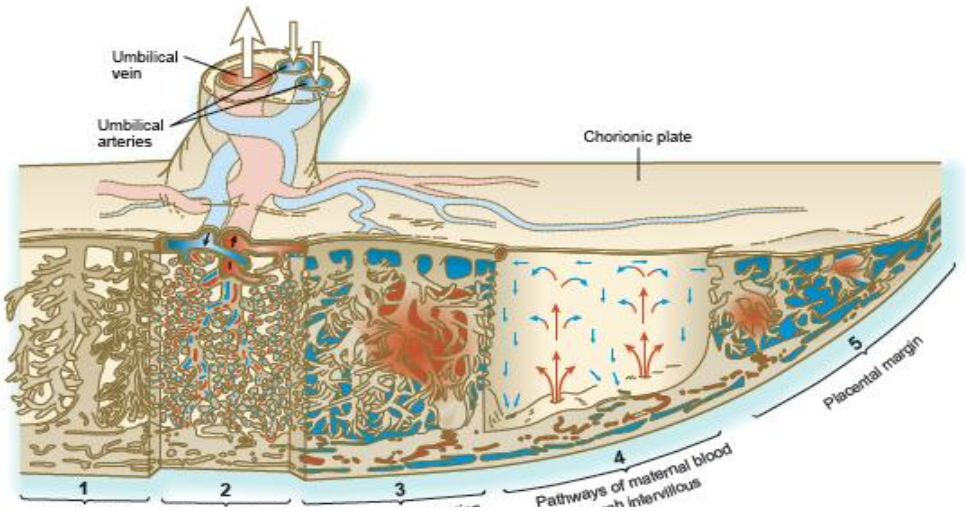

Figure 3: Structure and circulation of the mature human placenta. Blood enters the intervillous spaces from the open ends of the uterine spiral arteries. After bathing the villi, the blood (blue) is drained via endometrial veins [(4)].

The sum of all these layers constitutes the placenta, a temporary organ that allows the exchange of nutrients, gases and other metabolites between the mother and the fetus [(7)]. The

human placenta is classified as hemochorial because the fetal tissue is in direct contact with maternal blood existing, therefore, a juxtaposition of maternal and fetal circulations, without ever mixing the two [5, 8].

In early pregnancy stages, the placenta mediates embryo implantation into the uterus and produces hormones that prevent the end of the ovarian cycle. Once the embryo's implantation stage is succeeded, the placenta embraces many other important functions, being a crucial one the exchange of substances between the mother and the embryo that allow the latter to develop properly [9].

The degree of exchange surface is enlarged at the placenta membranes due to the presence of microvilli. The presence of mitochondria, ribosomes, pinocytotic vacuoles and lipid enclosures has also been shown, reinforcing the belief of intense functional activity of exchange and synthesis, at this surface [10].

The placental barrier is formed by cells that are interconnected by tight junctions, adherent junctions and desmosomes forming junctional complexes in a continuous line, regulating paracellular permeability and preventing the passage of macromolecules between the apical and basal cells poles. The frequency, position and dimensions of tight junctions are similar in all vessels, but seem to have different expression degrees [8]. These structural properties insure controlled passage of different substances.

The compounds can cross the cellular membranes via classical passive (facilitated diffusion, filtration, etc.) or active (carrier-mediated transport, endocytosis, etc.) transport systems [10]. In the case of simple diffusion, the transfer occurs without energy use and is dependent on the concentration gradient between maternal and fetal blood. Regarding facilitated diffusion, it is carrier-mediated but not dependent on energy. The transfer occurs down the concentration gradient, is inhibitable by structural analogs and is saturable [11]. There is also active transport, where the transfer occurs against an electrochemical or concentration gradient, requiring energy. It is, like facilitated diffusion, carrier-mediated, saturable, with possible competition between related molecules. There is also, in a minor scale, the transport of substances through endocytosis (phagocytosis or pinocytosis) and exocytosis, although it is probably the least understood transport process to date [11, 12]. Whether the case, it is a controlled traffic assured by specific membrane proteins. These systems include plasma membrane carriers such as ABC (**A**TP-**B**inding **C**assette) transporters and members of the SLC (**S**o**l**ute **C**arrier) family [5, 6].

The placenta also uses all these transporters as a mechanism, protecting the fetus from potentially harmful substances (Fig. 4).

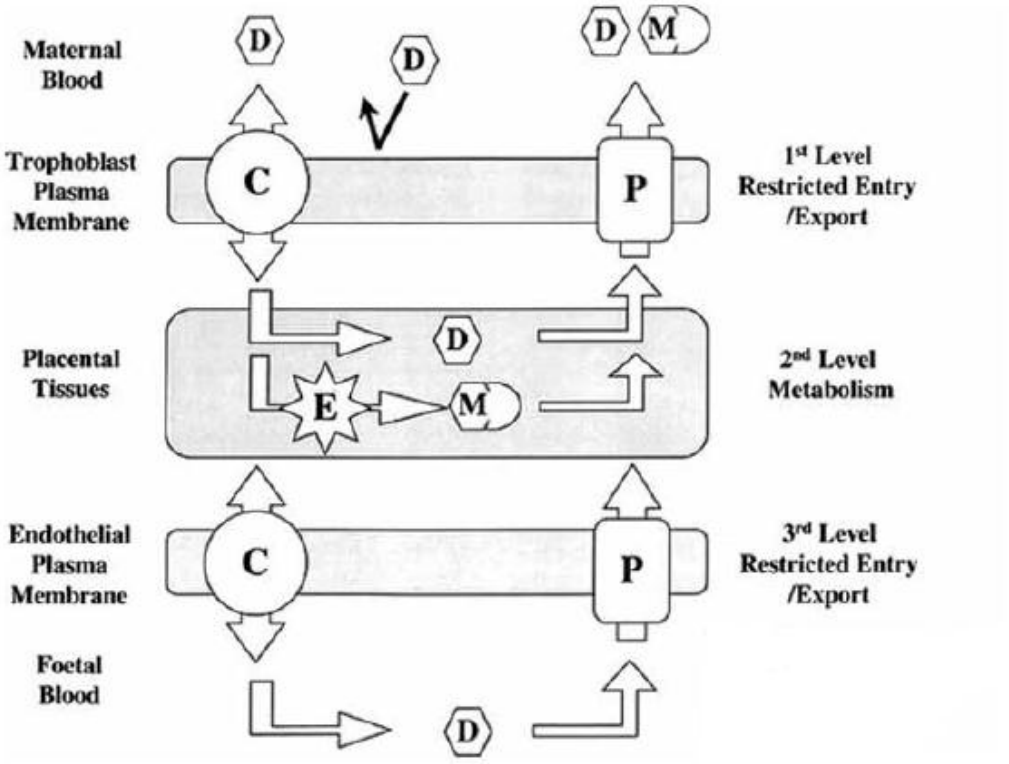

Figure 4: Three levels of protection involved in the human placental barrier for drugs [6].
C: Potentially bidirectional carriers. P: Export pumps. E: Metabolizing enzymes. D: Drug/Substrate.
M: Drug/Substrate metabolite

Despite this selectivity, the placenta is considered a highly permeable organ for a significant amount of substances [6] and has a major role in the transfer of nutrients that support embryonic and fetal growth and development (Fig. 5), as well as in the synthesis of several compounds, like proteins, hormones and other regulatory factors, that provide all the necessary conditions to insure all pregnancy processes [6, 9, 10]. Indeed, the placenta, and particularly the syncytiotrophoblast, is a very important endocrine organ, producing steroid hormones, like human chorionic gonadotropin (HCG), responsible for progesterone and estrogen production, chorionic somatomammotropin, and enzymes with critical role in hormones synthesis like 3β-hydroxysteroid dehydrogenase, aromatase and 17β-hydroxysteroid dehydrogenase, as well as human placental lactogen and small amounts of

chorionic thyrotropin and chorionic corticotropin. It also contains phase II enzymes like glutathione S-transferase α and π, epoxide hydrolase, *N*-acetyltransferase and sulfotransferases isoforms. [6, 9, 13]

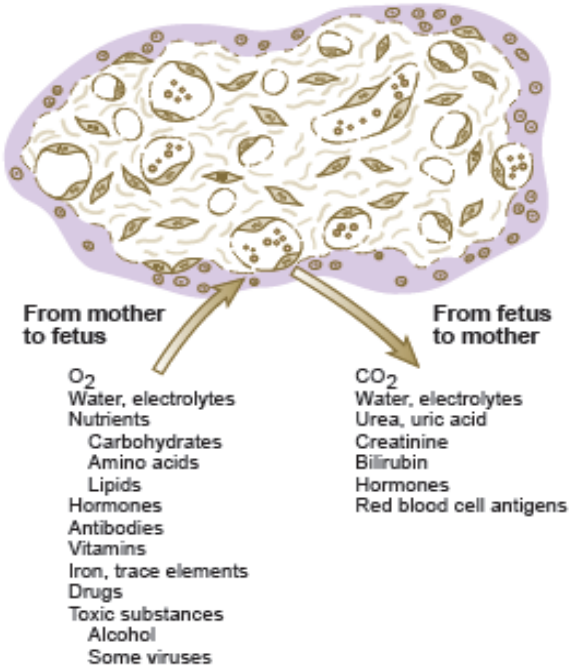

Figure 5: Placental exchange of substances between the mother and the fetus. [4]

It is also important to refer that as pregnancy progresses, the placental membranes change in composition and size, as well as the ability of certain substances to cross the placenta [5, 6]. Also, the membranes become thinner as pregnancy progresses, primarily due to partial disappearance of the cytotrophoblast. Despite this, in the human placenta, by the end of gestation the intensity of exchange decreases because of fibrinoid deposition on the exchange surface [9, 10].

9.2 Glucose transport at the placenta

Glucose is the primary and fundamental source of energy to all animal cells. As such, it is crucial that a proper amount of this hexose reaches the fetus, which has a significant absence of self-gluconeogenesis and, therefore, highly depends on the transplacental transfer of glucose from the mother [14-17]. The possible implications of deficient glucose quantities are mentioned later on in Introduction.

The maternal-fetal glucose transfer is regulated by several factors: glucose supply, placental glucose metabolism and placental glucose transporter density and activity. Glucose supply is determined by glucose concentration and blood flow. Glucose transfer across placenta barrier (intermembranous space) is a relatively rapid process compared to either the glucose supply or removal of glucose from the apical or basolateral membranes, respectively. Also, glucose transfer can be defined as a flow-limited phenomenon or, in other words, is limited by movement to and from the transfer site [16].

The supply of glucose by the placenta depends mainly on a facilitated diffusion transport mechanism and is regulated by a relatively complex set of mechanism that tends to keep its metabolism relatively constant [14, 15, 17-20]. Investigations reported back to the 80's decade have already proven the presence of Na^+- independent transporters belonging to a family of glucose transport proteins with similar kinetic characteristics – the GLUT family, a group of at least 12 isoforms (GLUT1 – GLUT12) of integral, transmembranar proteins, belonging to the group of solute carriers (SLCs) that gather a few common structural and metabolic characteristics: the presence of 12 membrane-spanning helices, seven conserved glycine residues in the helices, several basic and acidic residues at the intracellular surface of the proteins, two conserved L-tryptophan residues, two conserved L-tyrosine residues, selectivity for D- over L-glucose and sensitivity to inhibition by phloretin and cytochalasin B [21-26].

GLUT1 is considered the major glucose transporter isoform at the human placenta and also plays an important role in mediating implantation of the embryo. It is a membrane spanning glycoprotein containing 12 transmembranar domains with a single *N* – glycosylation site and its gene, SLC2A, is located on chromosome 1 (1p35 – 31.1). It has a catalytic turnover of ~1200/s and provides an efficient pathway for cellular import and export of glucose [19]. It is found at both the maternal - facing microvillus trophoblast membrane and the fetal – facing basal trophoblast membrane, with an approximately three-fold higher quantity in the microvillus membrane, compared to the basal [14-16, 23]. Also, the 6-fold larger surface area of

the microvillous covering leads to several times higher total transport capacity across the syncytial compared to the basal membrane. [14] For this reason, placental glucose transport is called “asymmetric”, since the maximal velocity (v_{max}) for sugar exit into sugar-free medium is not identical to the v_{max} for sugar entry into sugar-free cells.

This asymmetry has led to an important insight: the hypothesis that the basal membrane is the rate limiting step in transsyncytial transport of glucose [16]. Plus, studies have shown that the expression of GLUT1 in abnormal conditions is altered. More specifically, in diabetic human placenta, GLUT1 levels are increased while in intrauterine growth restriction GLUT1 levels are decreased [18, 19]. There are presently no specific GLUT1 inhibitors known. However, the inhibitors known for the GLUT family, cytochalasin B and phloretin, seem to be consider quite efficient, suggesting that GLUT1 ligand binding is compatible with a fixed site transport mechanism. In this type of mechanism, a ligand such as cytochalasin B that binds close to the endofacial sugar binding site does not eliminate the exofacial sugar binding site, unless occupancy of the endofacial binding site by the inhibitor reduces greatly the affinity of the exofacial site for glucose (Fig. 7) [19, 23, 27].

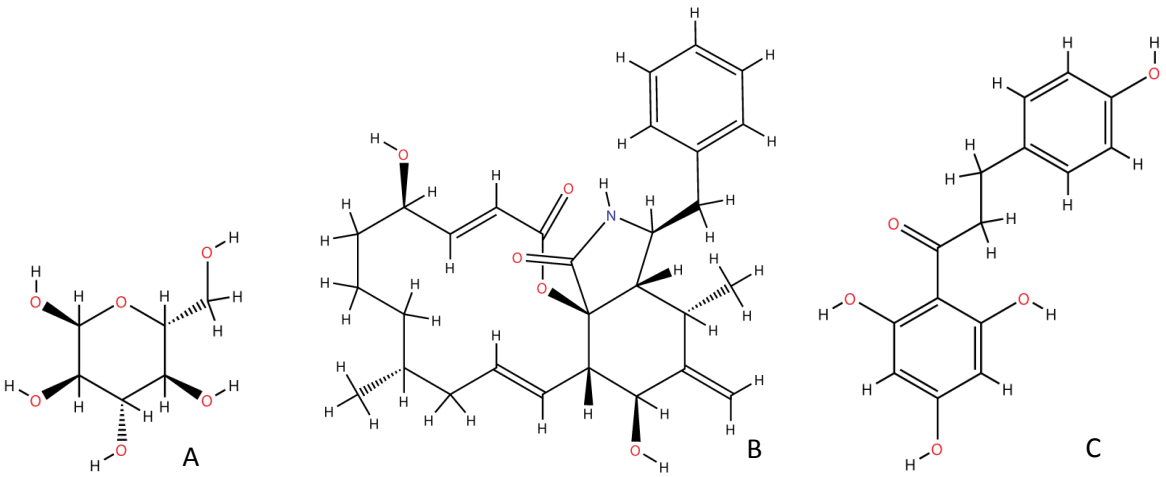

Figure 6: Molecular structure of D-Glucose (A), cytochalasin B (B) and phloretin (C), respectively [2].

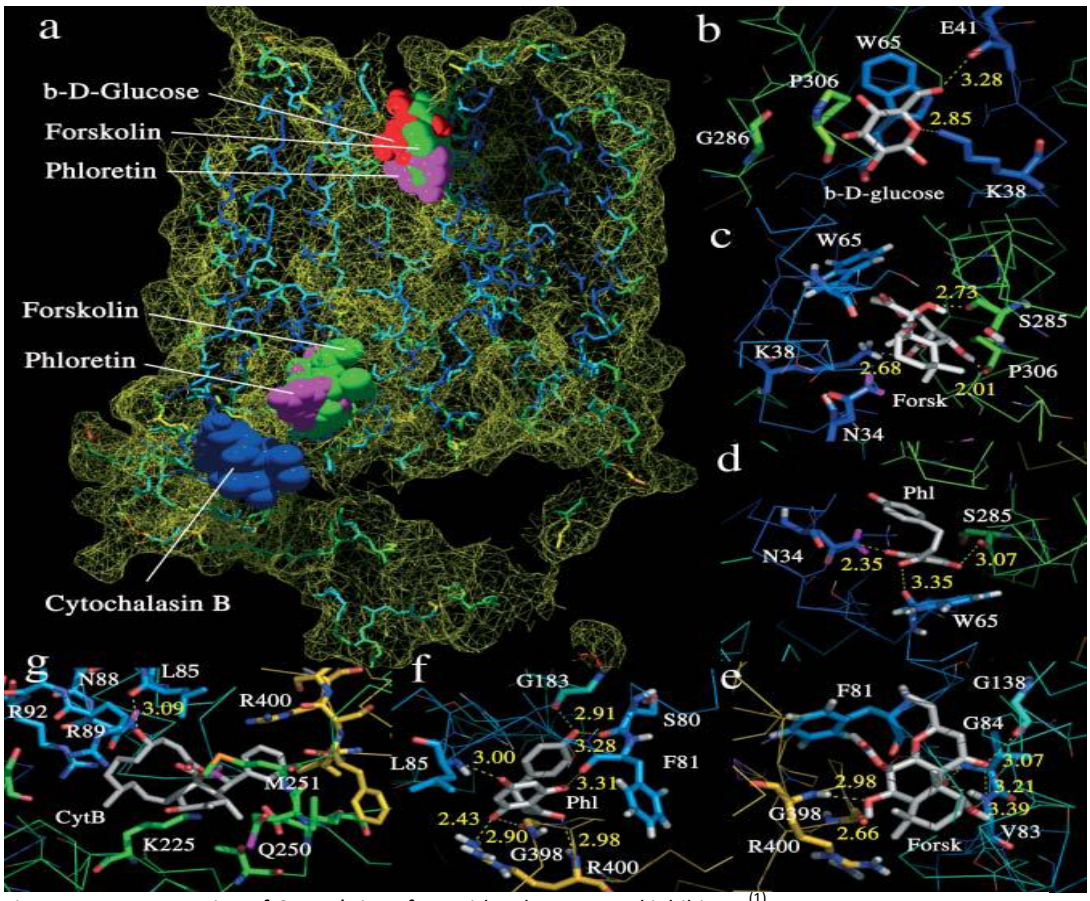

Figure 7: Representation of GLUT1's interface with substrates and inhibitors [1].

Although GLUT1´s expression has been established as the principal mediator of placental glucose transport, several studies investigated if other isoforms are also present at the human placental tissues and their role. These studies showed that GLUT3, GLUT4, GLUT9 and GLUT12 appear to be expressed at some extent [15, 16, 19, 22, 27-30].

GLUT4 is an insulin-sensitive isoform and has been reported as being present in Jar choriocarcinoma cells but at levels so low that an insignificant contribution to cellular glucose uptake was suggested [16]. Also, this isoform has not been identified in membranes from primary cultured syncytiotrophoblasts or cytotrophoblasts; so, it is unlikely that GLUT4 contributes for trophoblast glucose uptake *in vivo* [16]. In a study conducted by Araújo *et al*, in BeWo cells, uptake of an analogue of glucose was shown to be insulin-independent, which indicates that, even if present, GLUT4 probably has a minor role, if any, in glucose uptake at the placenta [27].

GLUT12 exhibits 29% homology with GLUT4 and, for that reason, it has been postulated that GLUT12 could be a second insulin-sensitive glucose transport system. Studies support the hypothesis that GLUT12 acts to facilitate glucose transport *in vivo* and its expression in

human placenta has been demonstrated by RT-PCR and Western blotting [28]. However, its immunoreactivity seems to be predominantly expressed in the syncytiotrophoblast and extravillous trophoblast at the first trimester of gestation, and GLUT12 does not seem to be found at syncytiotrophoblasts at term [28].

GLUT9 is a relatively recently cloned member of the GLUT family, and has been shown to exist as 2 splice variants, GLUT9a and GLUT9b, each with different targets at the membrane [30]. The placenta is one of the few tissues that express both variants at the mRNA level, suggesting a possible role for both GLUT9a and GLUT9b in placental hexose transport. GLUT9 transports both glucose and fructose but with close to 3-fold higher affinity for glucose [30].

Concerning GLUT3, studies are somehow contradictory, namely in relation to tissues in which it is expressed, as well as its levels of expression. Collectively, the results show that, although GLUT3 mRNA is distributed throughout villous tissue, GLUT3 protein appears to be expressed in vascular endothelium, and it is still not clear if GLUT3 protein is expressed at the syncytiotrophoblast layer. Some recent studies affirm that GLUT3 is indeed present at the syncytiotrophoblast layer but mainly during first trimester. Also, GLUT3 has been reported to be a GLUT isoform with a higher affinity for glucose than GLUT1. So, GLUT3 could have an important part in the glucose uptake by the fetus in circumstances associated with a decrease in glucose concentration. Interestingly, GLUT3 mRNA levels seem to be altered under certain stimuli, such as hipoxia [15, 19, 22, 29].

Table 1: Main glucose transporter isoform distribution at the human placenta [16, 31]

GLUT isoform	Protein	mRNA
GLUT1	Syncytiotrophoblast, cytotrophoblast, endothelium, vascular smooth muscle, stromal cells	Syncytiotrophoblast, cytotrophoblast, endothelium, vascular smooth muscle, stromal cells
GLUT3	First trimester: extravillous trophoblast, cytotrophoblast Third trimester: endothelium	First trimester: unclear Third trimester: syncytiotrophoblast, cytotrophoblast, endothelium
GLUT4	Stromal cells	Stromal cells
GLUT9	At term: GLUT9a: basolateral membrane of the syncytiotrophoblast At term: GLUT9b: microvillous membrane	At term: GLUT9a: basolateral membrane of the syncytiotrophoblast At term: GLUT9b: microvillous membrane
GLUT12	First trimester: extravillous trophoblast, cytotrophoblast, syncytiotrophoblast Third trimester: vascular smooth muscle, stromal cells	First trimester: extravillous trophoblast, cytotrophoblast, syncytiotrophoblast Third trimester: vascular smooth muscle, stromal cells

9.3 Oxidative stress at the placenta and Antioxidants

Oxidative stress is the term used to designate an imbalance between reactive oxygen species (ROS) and antioxidant levels in a cell, favoring the former [2, 31-33]. At homeostatic levels, ROS are implicated in diverse actions on cell function, like activation of redox-sensitive transcription factors and activation of protein kinases [2], regulation of vascular tone and functions controlled by O_2 concentrations, enhancement of signal transduction from many membrane receptors, like the antigen receptor of lymphocytes [32], among others.

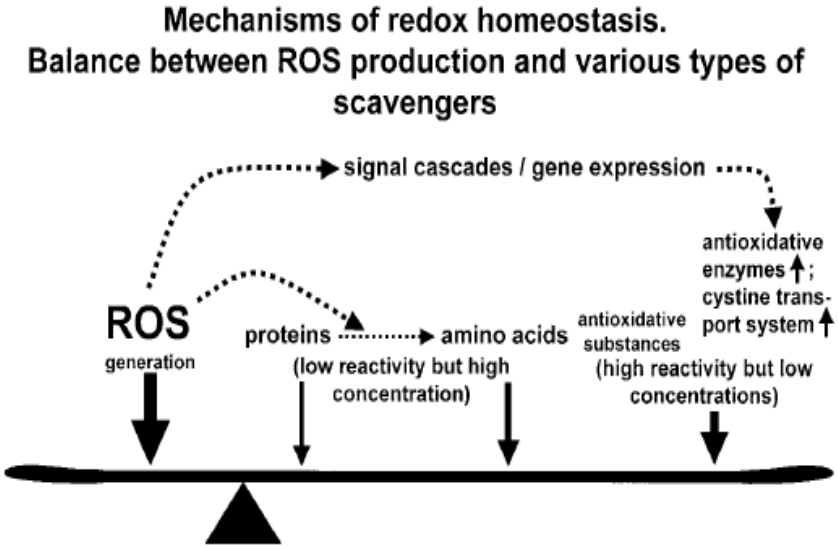

Figure 8: Mechanisms of redox homeostasis. Balance between ROS production and various types of scavengers. The steady-state levels of ROS are determined by the rate of ROS production and their clearance by scavenging mechanisms [8].

However, when in excess, ROS can induce cell injury and a chronic inflammatory state that can trigger a cascade of free radical reactions, promoting secondary ROS generation and resulting in cellular modification and damage in DNA, carbohydrates, proteins and polyunsaturated fatty acids (Table 2).

Table 2: Some common biomarkers of oxidative stress used in the study of human diseases (38)

Table 2: Some common biomarkers of oxidative stress used in the study of human diseases [34]	
DNA	Aldehyde/other base adducts Nitrated/deaminated bases Oxidized bases
Lipids	Chlorinated/nitrated lipids (isoprostanes, isoleukotrienes) Oxysterols (aldehyde) Peroxides (malondialdehyde, 4-hydroxy-2-nonenal, acrolein)
Proteins	Aldehyde adducts Carbonyl group formation Nitrated/chlorinated Tyr, Trp, Phe Oxidized Tyr, Trp, His, Met, Lys, Leu, Ileu, Val Protein peroxides/hydroxides SH (thiol) oxidation

This oxidative injury follows a general pattern that involves free thiol oxidation and formation of disulphide proteins, depletion of the ATP pool, free cytosolic Ca^{2+} increment, disintegration of cytoskeleton, increased membrane peroxidation, release of cytosolic compounds and DNA damage [33, 35]. Examples of conditions associated with increase oxidative state include cellular aging, brain dysfunction and neurodegenerative diseases, atherosclerosis, cancer, diabetes, rheumatoid arthritis and cardiovascular and renal diseases [32, 36-38].

Reactive oxygen species include free radical intermediates, such as the superoxide anion radical $O_2^{\bullet -}$ (under physiological conditions it is the most common [2]), hydroxyl radical $HO^{\bullet}$, peroxyl radical $ROO^{\bullet}$, alkoxyl radical $RO^{\bullet}$ and hydroperoxyl radical $HO^{\bullet}_2$, and also non-radical intermediates, such as hydrogen peroxide (H_2O_2), ozone (O_3), hypochlorous acid (HOCl), peroxynitrite ($ONOO^-$) and singlet oxygen ($^1O_2$), with high instability due to the existence of one, or more, unpaired electrons [34, 35, 38]. ROS can be generated from multiple mechanisms, such as:

- Normal metabolic reactions, such as redox reactions during cell respiration. The oxygen's reduction to water implies a 1-2% electron leakage, generating $O_2^{\bullet -}$ at the ubiquinone and NADH dehydrogenase (complex I), as well in complex III;
- Radiation, exciting UV rays and ionizing X rays;
- Xenobiotics and drug metabolism;
- The activity of monoamine oxidase, which deaminates biogenic amines. This mechanism occurs at the outer membrane of the mitochondria, and is associated to large H_2O_2 production;

- In purines catabolism and formation of uric acid, by xanthine oxidase, a superoxide producing enzyme;
- During an inflammatory response, the production of H_2O_2 and $O_2^{\bullet -}$ increases greatly in cells like polymorphonuclear cells, eosinophils, monocytes, Kupffer cells and macrophages, thanks to a highly specialized NADPH-dependent oxidase system located in the outer surface of cell membrane, coupled to the action of superoxide dismutase (SOD) [2, 39].
- In the endoplasmic reticulum (ER), where a significant amount of superoxide is formed, during protein folding. In this process, the formation of disulphide bonds is an oxidative process, since it is due to the oxidation of sulphydryl groups of cysteine residues [2, 39, 40].

At the placenta, ROS also seem to have important roles. During placental development, oxygen levels are relatively low, due the unfully established maternal intraplacental circulation, which is believed to be the reason why the embryo is particularly protected from oxygen free radicals at that time. These low levels are essential for normal placental angiogenesis, promoted by hypoxia-induced transcriptional and post-transcriptional regulation of angiogenic factors, like the vascular endothelial growth factor and placental growth factor [41]. Once the maternal intraplacental circulation is fully formed (towards the end of the first trimester) the O_2 concentration triplicates and, with it, so does ROS levels, particularly at the syncytiotrophoblastic layer [2, 42]. Also, the placental itself is a source of ROS [43].

Besides their inherent instability, ROS have a very short half-life (seconds) because of the efficiency of the antioxidant defense of the cells.

Antioxidants are substances that, at relatively low concentrations, compete with other substrates susceptible to oxidation, delaying or inhibiting the oxidation of these substrates. They are, therefore, one of the cells' defense mechanisms against ROS [32, 38]. There are enzymatic and non-enzymatic antioxidants [2]. Enzymatic antioxidants comprehend proteins that have a transitional metal in their core, capable of different valence states as they transfer electrons during the detoxification process [2]. Antioxidant enzymes play a very important role in the response of trophoblasts to the significant increase in oxidative stress levels resulting from the perfusion of the intervillous space with maternal blood [41]. Examples of these compounds are glutathione peroxidase, glutathione catalase and two isoforms of superoxide dismutase (SOD), the manganese form, which is present in the mitochondria, and

the copper and zinc form, present in the cytosol. These two forms convert superoxide to hydrogen peroxide that is then broken down to water by catalase or glutathione peroxidases. 1-Cys peroxiredoxin (peroxiredoxin 6), peroxiredoxin 2 (thioredoxin peroxidase) and peroxiredoxin 1 (thioredoxin peroxidase 2) are also associated with several biological processes, among them oxidants detoxification [2, 32, 38, 41, 44-46].

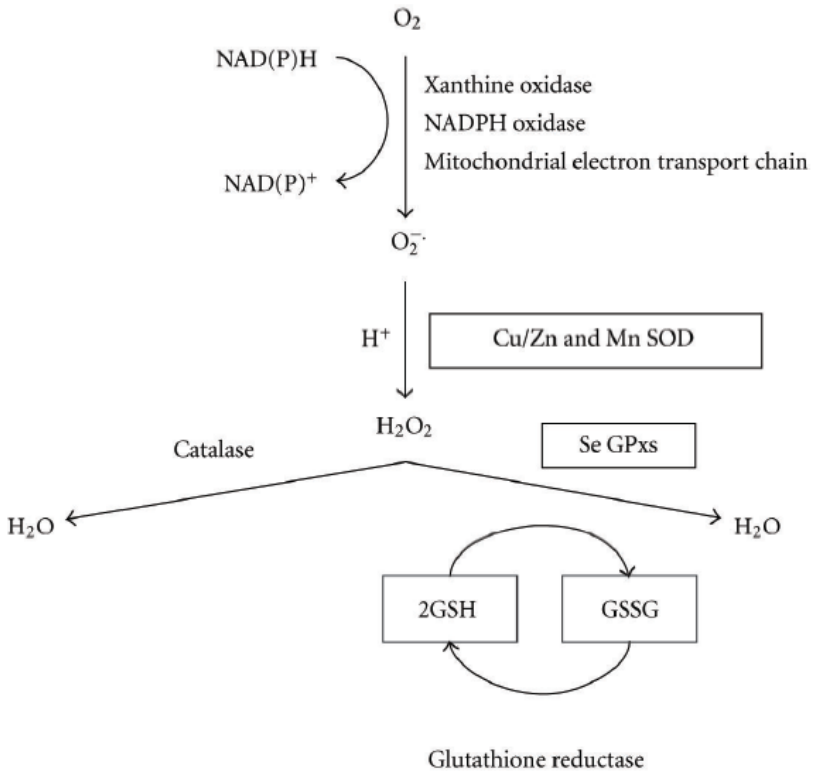

Figure 9: Major pathways of ROS generation and metabolism. Superoxide can be generated by specialized enzymes, such as the xanthine or NADPH oxidases, or as a byproduct of cellular metabolism, particularly the mitochondrial electron transport chain. Superoxide dismutase (SOD), both Cu/Zn and Mn SOD, then converts the superoxide to hydrogen peroxide (H_2O_2) which has to be rapidly removed from the system. This is generally achieved by catalase or peroxidases, such as the selenium-dependent glutathione peroxidases (GPx) which use reduced glutathione (GSH) as the electron donor [3].

Non-enzymatic defenses include thiol compounds (glutathione (GSH)), lipoic acid, thioredoxin that needs thioredoxin redutase to be converted back to its reduced form) and ceruloplasmin and transferrin, that by sequestering free iron ions inhibit Fenton reactions and the production of $OH^{\bullet}$. It is, however, important to refer that all of these compounds have

low specific antioxidant activity (on a molar basis) but greatly contribute to the overall ROS scavenging activity when present in high concentrations [2, 32, 38, 45, 47].

Besides the antioxidants already mentioned, there are many other compounds that provide beneficial outcomes and can be found in food and nutritional supplements.

Ascorbic acid (vitamin C) and α-tocopherol (vitamin E), for example, are two vitamins that act in concert, with the first being necessary to the regeneration of the reduced form of the latter, which is why this is called an antioxidant network (Fig. 10). Vitamin C, or ascorbic acid, is an essential water-soluble vitamin widely found in fruit and vegetables and has important roles in collagen synthesis, wound healing and prevention of anaemia, besides its importance in ROS scavenging. α-Tocopherol is a lipid-soluble vitamin that acts at lipid membranes. Because it possesses an hydrophobic tail, it tends to accumulate within the interior of lipid membranes, acting as an important chain-breaker, as it reacts with lipid peroxyl radicals about four times faster than they can react with adjacent fatty acid side chains constituting, in this way, a crucial defense against ROS at biological membranes [2, 48]. Besides the antioxidant properties, vitamin E presents other effects, due to specific interactions with enzymes or transcription and specifically enhances the effect of ascorbic acid on cells [48]. It is found in cereals and seed oil [3].

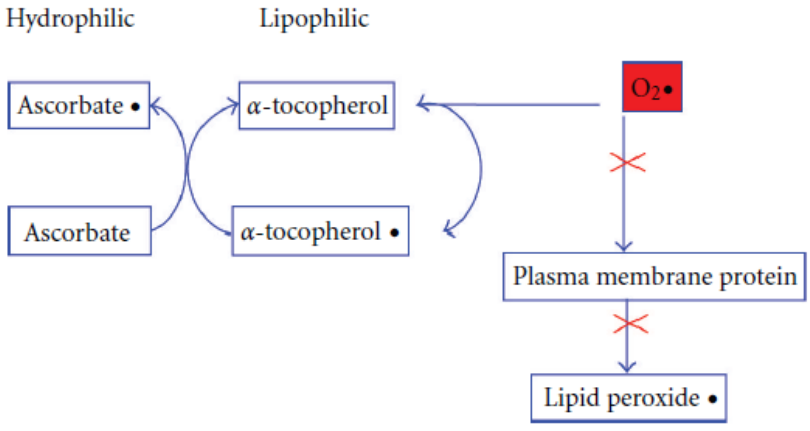

Figure 10: Synergistic mechanisms of vitamin C (ascorbic acid) and vitamin E (α-tocopherol) to prevent lipid peroxidation by O2• (oxygen free radical) [7].

Resveratrol, quercetin, epigallocatechin-3-gallate, β-carotene and *N*-acetylcysteine are other examples of natural antioxidants [27, 34, 35, 47]. The first three belong to a class of compounds

called polyphenols, which constitute one of the most numerous and widely distributed groups in the plant kingdom. Polyphenols are products of secondary metabolism of plants and, chemically, they are characterized by containing, linked to a benzoic ring, at least two hydroxyl groups. According to the number of phenolic groups contained or the structural elements that bind the rings to one another, polyphenols can be divided into at least ten classes [49]. Their antioxidant character provides a vast metabolic activity and they have been related to decrease in cardiovascular disease and atherosclerosis, the risk of Alzheimer's disease development and even in prevention of some cancers, as well as in cellular aging delay [50, 51].

9.4 The project

Nutrition during early development is associated with proper offspring's growth, organ development, body composition and body functions. It also implicates long-term effects on health and morbidity and mortality risk in adulthood, as well as on the development of neural functions and behavior, a phenomenon called 'metabolic programming' [52]. The response of the fetus to the environmental insults during the prenatal period is associated with increased susceptibility of the offspring to cardiovascular diseases, metabolic syndrome, hypertension, type II diabetes and obesity [53, 54].

So, it becomes fundamental to understand which conditions modulate the placental uptake of critical nutrients such as glucose. For example, although the fetus is known to have considerable capacity to metabolically adapt to acute and chronic changes in glucose supply, lower or higher maternal blood glucose levels can lead to alterations in fetal growth and weight [55]. Also, previous studies from the group showed that several bioactive compounds, as well as some drugs of abuse, may modulate the apical uptake of glucose at the placenta [27, 56]. According to several studies, ABC and SLC transporters are able to transport not only nutrients but also drugs and xenobiotics, which mean that the xenobiotics may compete with the physiological substrates of the placental transporters and interfere with the delivery of nutrients such as glucose to the fetus [6, 9]. And, as gestation progresses, there is a higher possibility for xenobiotics, among other substrates, to enter fetal tissues leading to potential effects on fetal development because cytochromes P450 like CYP1, CYP2 and CYP3, responsible for the detoxification of drugs and toxins, tend to decline in expression and activity from the first trimester to the second and third trimesters [5, 6]. Another important fact is that some compounds may enter the placenta and be then metabolized into toxic substrates leading also to possible negative implications to a proper fetal development. It has also been proven that several drugs of abuse influence the perfusion pressure of the placenta [10].

As pregnancy progresses, morphological and biochemical alterations take place at the placenta, as already mentioned. One of the most significant changes is oxygen levels. Initially, the placenta develops at a low oxygen environment, with a pressure around 20 mmHg [41]. This favors cell proliferation and angiogenesis in the placenta and organogenesis in the embryo. Once the intervillous circulation is established, the oxygen tension rises. The placenta then adapts to this increase by modulating hypoxia-inducible factor 1α (HIF-1α) and increasing cellular antioxidants levels [41]. Under normal conditions, this adaptation is

favorable to fetal development. For example, some studies suggest that NAD(P)H oxidase can act as an "oxygen sensor", regulating differentiation from cytotrophoblast to syncytiotrophoblast when oxygen tension increases, or that VEGF-A (vascular endothelial growth factor A) and metalloproteins are sensitive to oxidative stress. Also, superoxide activates cytokine synthesis and, therefore, may play a role in maternal inflammatory state that characterizes normal pregnancy [47]. So, it is understandable that aberrations in these modifications and adaptations predisposes placental villi to high oxygen tension, hypoxia, hypoxia-reoxygenation and mechanical injury in all different stages of the pregnancy, all of which are implicated in pregnancy complications [41].

Several studies have been conducted for the last two decades that relate increased oxidative stress levels to several pregnancy pathologies, including spontaneous abortion, idiopathic recurrent pregnancy loss, defective embryogenesis, drug-induced teratogenicity, preeclampsia, intrauterine growth restriction and minor congenital abnormalities, as well as to future diseases in adulthood, such as obesity, diabetes mellitus and hypertension [32, 40-43, 57-59]. For example, preeclampsia by itself is a state of oxidative stress, with several studies reporting a decrease of placental antioxidant capacity and an increase in the source of ROS in a preeclamptic placenta, which is likely to be a combination of increased mitochondrial generation and synthesis through xanthine oxidase and NAD(P)H oxidase [47]. Another example is fetal growth restriction, which is recognized as a major cause of perinatal morbidity and mortality.

From the preceding description, it can be seen that oxidative stress may induce a wide range of cellular responses depending upon the severity of the insult and the compartment in which the ROS are generated. Some of the more major signaling pathways involved and potential outcomes are presented in Fig. 11.

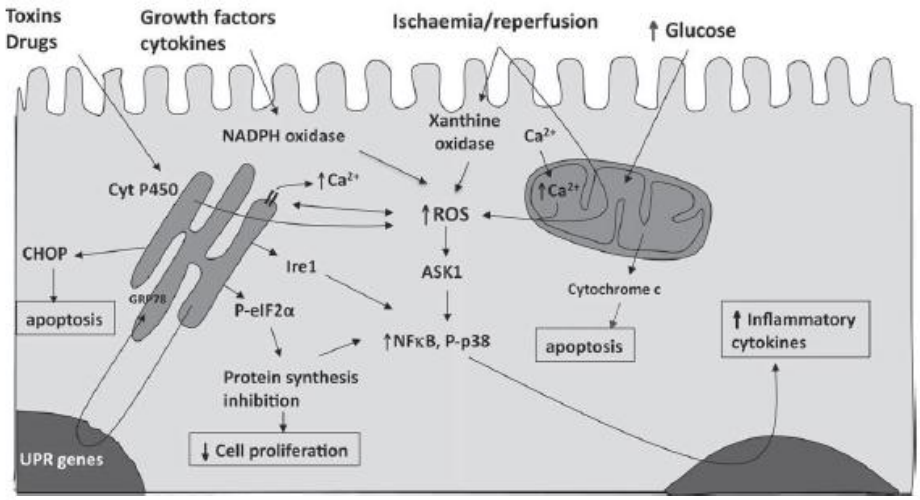

Figure 11: How reactive oxygen species may be generated within the syncytiotrophoblast, and the main consequences for the function of the tissue. CHOP (C/EBP homologous protein); NADP (nicotinamide adenine dinucleotide phosphate); ROS (reactive oxygen species); UPR (unfolded protein response) [2]

Besides the increase in placental concentration of ROS due to placental metabolism, pregnant women can be exposed to environmental oxidative stress inducers, as a part of their lifestyle or diet, smoking, drugs and alcohol consumption. In biochemical terms, this represents an even more accentuated increase of ROS levels. As already mentioned, excessive ROS levels are usually synonymous of increased health risk for the mother and the fetus.

So, knowledge on the placenta's dynamics becomes fundamental, in order to understand which conditions and substrates, or lack of such, can imply a pathological risk to the fetus. With this in mind and taking that very little is known about the subject, the purpose of this study was to find out if the uptake of glucose, the fetus' primary source of energy, would be compromised under oxidative stress conditions. For such, a proper cellular model representative of the human placenta dynamics was necessary and the BeWo cell line was chosen.

BeWo cells derive from a human choriocarcinoma and are a trophoblastic cell line that forms a confluent and consistent monolayer. This is an essential condition to investigate the processes of regulation/distribution of several compounds between maternal and fetal compartments. BeWo are stable, i.e., have low spontaneous fusion rate, are relatively easy to maintain by passage, grow into confluent monolayer, with regular microvilli on the apical surface, in a short period of time (about 5 to 7 days) and own the important feature of displaying morphological properties and biochemical marker enzymes that are common to

the normal trophoblats. Also, they exhibit polarized transcellular transport of transferrin, serotonin and monoamine uptake systems and, when treated with adenosine 3',5'-cyclic monophosphate or forskolin, differentiate and exhibit morphological characteristics similar to the fusion of cytotrophoblasts into a syncytia in primary culture [20, 60, 61]. For all these reasons, BeWo is the most extensively used cell cellular model for villous trophoblasts investigations [60], including analysis of hypoxia-induced responses in the syncytialization of human placenta [44], studies on syncytial fusion and expression of syncytium-specific proteins [62], studies on transport of xenobiotics and drugs of abuse [27], evaluation of therapeutic agents [60, 61], studies on the link between certain compounds and some pregnancy pathologies, among many others. BeWo cells constitute an excellent alternative for human cytotrophoblasts because the latter tend to spontaneously differentiate into syncytiotrophoblasts, but not forming the needed confluent and consistent monolayer for transcellular transport processes [20, 60].

In order to study the effect of oxidative stress upon glucose uptake, *tert*-butylhydroperoxide (tBOOH; $C_4H_{10}O_2$) was used. tBOOH is an oxidant organic compound that can access biological membranes and has been extensively used as an oxidative stress inducer in a variety of systems [63]. The genotoxicity of this compound increases due to reactions related to transition metals, resulting in the formation of different ROS, including H_2O_2 [35, 63]. Among proposed mechanisms of action for tBOOH, homeostatic alteration of intracellular Ca^{2+}, followed by depletion of glutathiones and proteins with thiol groups, breakdown of DNA chains, lipid peroxidation and production of *tert*-butoxil radicals have been referred [35, 64].

10 Objectives

The purpose of this project was to investigate, using the BeWo cell line, the effect of oxidative stress upon the absorption of glucose at the placenta. For that, the inherent objectives were:

1. To quantify some oxidative stress biomarkers, in BeWo cells, after exposure to increasing concentrations of *tert*-butylhydroperoxide (tBOOH) for 24h:
   1.1. Total glutathione (GSx), oxidized glutathione (GSSG) and reduced glutathione (GSH) levels;
   1.2. Lipid peroxidation;
   1.3. Carbonylated proteins;
2. To evaluate cellular integrity, in BeWo cells, after exposure to increasing concentrations of tBOOH for 24h;
   2.1. Cellular viability;
   2.2. Cellular proliferation;
3. To quantify ^{3}H-2-D-glucose (^{3}H-DG) uptake, by BeWo cells, after 24h of exposure to tBOOH at the concentration chosen as optimal to induce stress, taking points 1 and 2:
   3.1. To evaluate the time-course of ^{3}H-DG uptake;
   3.2. To evaluate the kinetics of uptake, K_m and V_{max};
   3.3. To evaluate the pharmacological characteristics, by using specific inhibitors;
4. To quantify the mRNA levels of the glucose selective transporter GLUT1, by qRT-PCR, in BeWo cells after 24h of exposure to tBOOH at the concentration chosen as optimal to induce stress, taking points 1 and 2.
5. To quantify lactate levels, in BeWo cells, after 24h of exposure to tBOOH at the concentration chosen as optimal to induce stress, taking points 1 and 2.
6. To quantify ^{3}H-2-D-glucose (^{3}H-DG) apical-to-basolateral transepithelial transport across BeWo cells, after 24h of exposure to tBOOH at the concentration chosen as optimal to induce stress, taking points 1 and 2.

11 Materials and Methods

11.1 Materials

2-[1,2-^{3}H(N)]-deoxy-D-glucose - specific activity 60 mCi/mmol (American Radiolabeled Chemicals, St. Louis, MO, USA); BSA (albumin from bovine serum), acetic acid sodium salt, chelerythrine chloride, collagen type I, cytochalasin B (from Diechslera dematioidea), decane, DTNB (5,5'-dithiobis(nitrobenzoic) acid), DNP (2,4-dinitrophenylhydrazine), EGCG [(–) epigallocatechin-3-gallate], FCS (fetal calf serum), GSH reductase, Ham's F12K medium (Kaighn's modification), guanidine hydrochloride, LY-294002 hydrochloride (2-(4-Morpholinyl)-8-phenyl-1(4H)-benzopyran-4-one hydrochloride), NAC (N-acetyl-L-cysteine), NADPH (β-nicotinamide adenine dinucleotide 2′-phosphate reduced tetrasodium salt hydrate), NADH (β-Nicotinamide adenine dinucleotide, reduced disodium salt hydrate), quercetin dihydrate, phloretin, resveratrol, sodium pyruvate, phenol red sodium salt, sulforhodamine B, tBOOH (*tert*-butylhydroperoxide solution) 2-thiobarbituric acid, trichloroacetic acid sodium salt, Tris-HCl and 2-vinylpyridine (Sigma, St. Louis, MO, USA); D(+)-glucose, DMSO (dimethylsulfoxide), ethylacetate, perchloric acid and Triton X-100 (Merck, Darmstadt, Germany); ethanol (Panreac, Barcelona, Spain).

The drugs to be tested were dissolved in water, decane, methanol or DMSO. The final concentration of the solvents in the buffer and culture medium was 1% (v/v).

11.2 Methods

11.2.1 BeWo cell culture

The BeWo cell line was obtained from the *American Type Culture Collection* (ATCC CCL-98, Rockville, MD, EUA) and was used between passage numbers 34 and 65. The cells were maintained in a humidified atmosphere of 5% CO_2-95% air and were grown in Ham's F12K Medium, containing 2.5 g/l sodium bicarbonate, 10% heat-inactivated fetal calf serum, and 1% antibiotic/antimycotic solution. Culture medium was changed every 2 to 3 days and the culture was split every 7 days. For sub-culturing, the cells were removed enzymatically (0.25% trypsin-EDTA, 5 min, 37 °C), split 1:3, and sub-cultured in plastic culture dishes (21 cm2; Ø 60 mm; Corning Costar, Corning, NY, USA). For oxidative stress markers and transport studies, BeWo cells were seeded on collagen coated 12-well (3.6 cm^2; Ø 21 mm; TPP®) or 24-well (2 cm^2; Ø 16 mm; TPP®) plastic cell culture clusters and were used after 5-7 days in culture (90-100% confluence). At that moment, each square centimeter contained about 60

µg cell proteins. For transepithelial transport studies, cells were seeded on collagen-coated Transwells® (1.12 cm^2; Corning Costar, Corning, NY, USA) and were used after 8-10 days.

11.2.2 Incubation of BeWo cells with *tert*-butylhydroperoxide (tBOOH)

Before each experiment, the cell culture medium was removed and each well was incubated with serum free culture medium for 24h, at 37°C, in the absence or presence of tBOOH.

11.2.3 Evaluation of tBOOH effect on cell integrity

11.2.3.1 Cellular viability (quantification of extracellular LDH activity)

Cells were seeded on 24-well plates and submitted to treatment with tBOOH (1, 3, 10, 30, 100, 300 and 1000 µM). After treatment, cellular leakage of the cytosolic enzyme lactate dehydrogenase (LDH) into the extracellular medium was measured spectrophotometrically by measuring the decrease in absorbance of NADH during the reduction of pyruvate to lactate, as described by Bergmeyer and Bernt [65].

11.2.3.2 Cellular proliferation (sulforhodamine B (SRB) assay)

Cells were seeded on 24-well plates and submitted to treatment with tBOOH (1, 3, 10, 30, 100, 300 and 1000 µM). After treatment, 62.5 µl of ice-cold 50% (w/v) TCA were added to the culture medium on each well to fix cells (1h at 4°C in the dark). The plates were then washed five times with tap water to remove TCA. Plates were air-dried and then stained for 15 min with 0.4% (w/v) SRB dissolved in 1% (v/v) acetic acid. SRB was removed and cultures were rinsed four times with 1% (v/v) acetic acid to remove residual dye. Plates were again air-dried and the bound dye was then solubilized with 375 µl of 10 mM Tris.NaOH solution (pH 10.5). The absorvance of each well was determined at 540 nm [66].

11.2.4 Evaluation of tBOOH-induced oxidative stress

The extent of oxidative stress induced by tBOOH was indirectly evaluated by measuring total (GSx), oxidized (GSSG) and reduced (GSH) glutathione levels, protein carbonyl groups and generation of lipid peroxidation products.

11.2.4.1 Measurement of total (GSx), oxidized (GSSG) and reduced (GSH) glutathione levels

Cells were seeded on 24-well plates and submitted to treatment with tBOOH (10, 30 and 100 µM). Afterwards, measurements of intracellular GSx levels were carried out according to a previously published method [67]. Briefly, cells were scraped and proteins precipitated with perchloric acid 5%, then centrifuged for 10 min at 4°C and the supernatant was neutralized with an equimolar solution of $KHCO_3$. GSx contents were measured by the rate of colorimetric change of 0.7 mM 5, 5-dithiobis (nitrobenzoic acid) at 415 nm in the presence of 0.4 U of GSH redutase and 0.24 mM NADPH, using a microplate reader. GSSG was also quantified, using 2-vinylpiridine to block free SH groups. GSH levels were calculated according to the following reaction: GSx = GSH + 2 GSSG.

11.2.4.2 Measurement of lipid peroxidation (TBARS assay)

Cells were seeded on 12-well plates and submitted to treatment with tBOOH (10, 30 and 100 µM). The extent of lipid peroxidation, determined as the formation of malondialdehyde occurring after the breakdown of polyunsaturated fatty acids, was measured by the thiobarbituric acid reactive substances (TBARS) assay. [70] Briefly, 300 µl of cell suspension was precipitated with 200 µl of 50% trichloroacetic acid (TCA) and centrifuged for 1 min at 6000 rpm. 300 µl of the supernatant were added with equal volume of 1% thiobarbituric acid and the resulting mixture was heated during 40 min at 95°C. The absorvance was measured at 535 nm after the mixture was cooled.

11.2.4.3 Measurement of carbonylated proteins

Cells were seeded on 12-well plates and submitted to treatment with tBOOH (100 µM). Carbonyl (CO) groups (aldehydes and ketones) are produced on protein side chains when

they are oxidized. Protein carbonyl content is the most used marker of protein oxidation [50]. Detection of protein carbonyl groups involves their reaction with 2,4-dinitrophenylhydrazine (DNPH), which leads to the formation of a stable 2, 4-dinitrophenyl (DNP) hydrazone product, followed by the spectrophotometric quantification of the acid hydrazones [72]. Briefly, carbonyl content was measured in the resulted pellet that was treated with 0.5 ml of 2, 4-dinitrophenylhydrazine (10 mM in HCl 2 M) or 0.5 ml of HCl 2 M for the blank. Samples were incubated for 1h at room temperature, vortexing every 10 min. 0.5 ml of TCA 20% was added to each tube which was allowed to stand for 15 min at 4°C. The resultant pellet was washed 3 times with ethanol-ethyl acetate (1:1), centrifuged at 13000 rpm for 2 min at 4°C and dissolved in 1 ml guanidine 6 M overnight. The solution was then centrifuged at 3000 rpm for 15 min. Absorbance was read at 340 nm and carbonyl content was calculated using the extinction coefficient of 22 000 M^{-1} cm^{-1}.

11.2.5 Determination of ^{3}H-2-deoxy-D-glucose (^{3}H-DG) uptake

Transport experiments were performed in glucose-free HEPES-buffered solution (GF-HBS) containing NaCl 140 mM, KCl 5 mM, $CaCl_2$ 1 mM, $MgSO_4$ 2.5 mM, HEPES 20 mM and pH 7.4. Initially, the culture medium was aspirated and the cells were washed with buffer at 37°C; then the cell monolayers were pre-incubated for 20 min in buffer at 37°C in the absence or presence of tBOOH and the testing compounds. Uptake was initiated by the addition of 0.2 ml buffer at 37°C containing 50 nM ^{3}H-DG, in the absence or presence of tBOOH and the testing compounds. Incubation was stopped after 120 min (except in the time-course experiments) by removing the incubation medium and rinsing the cells with 0.5 ml ice-cold buffer. The cells were then solubilized with 0.3 ml 0.1% (v/v) Triton X-100 (in 5mM Tris–HCl, pH 7.4), and placed at 4°C overnight. Radioactivity in the cells was measured by liquid scintillation counting.

11.2.6 Protein determination

The protein content of cell monolayers was determined as described by Bradford method [68] using serum albumin as standard.

11.2.7 Quantitative reverse transcription real-time-PCR (qRT-PCR)

Total RNA was extracted from BeWo cells using the Tripure® isolation reagent, according to the manufacturer's instructions (Roche Diagnostics, Germany). Before cDNA synthesis, total RNA was treated with DNase I (Invitrogen Corporation, CA, USA) according to manufacturer's instructions, and 10 µg of resulting DNA-free RNA were reverse transcribed using Superscript Reverse Transcriptase II and random hexamer primers (Invitrogen Corporation) in 40 µl of final reaction volume, according to the manufacturer's instructions. Resulting cDNA was treated with RNase H (Invitrogen Corporation) to degrade unreacted RNA. For the quantitative real-time PCR, 2 µl of the 40 µl reverse transcription reaction mixture were used. For the calibration curve, BeWo standard cDNA was diluted in five different concentrations. The primers pairs used for amplification were: 5'-GGT CAA GGT CGC AAG C-3' (forward) and 5'-GGG CAT ATC CTA CAA CAA ACT-3' (reverse) for housekeeping hypoxanthine-guanine phosphoribosyltransferase (HPRT) and 5'- GAT GAT GCG GGA GAA GAA GGT-3' (forward) and 5'- ACA GCG TTGA TGC CAG ACA G-3' (reverse) for facilitative glucose transporter 1 (GLUT1).

Real-time PCR was carried out using a LightCycler (Roche, Nutley, NJ, USA). 20 µl reactions were set up in microcapillary tubes using 0.5 µM of each primer and 4 µl of SYBR Green master mix (LightCycler FastStart DNA MasterPlus SYBR Green I, Roche). Cycling conditions were as follows: denaturation (95°C for 5 min), amplification and quantification (95°C for 10 s, annealing temperature (AT) for 15 s, and 72°C for 10 s, with a single fluorescence measurement at the end of the 72°C for 10 s segment) repeated 50 times, a melting curve program ((AT + 10)°C for 15 s and 95°C with a heating rate of 0.1°C/s and continuous fluorescence measurement), and a cooling step to 40°C (30 s). Annealing temperatures (AT) and sequence of primers are indicated in Table 1. Data were analyzed using LightCycler® 4.05 analysis software (Roche, Mannheim, Germany).

11.2.8 Lactate measurements

Lactates measurements were based on the oxidation of L-lactate (final product in anaerobic glycolysis) to pyruvate and hydrogen peroxide by lactate oxidase. The enzyme peroxidase, in the presence of a hydrogen donor, converts hydrogen peroxide in water and, hence, the 4-aminoantipirine in a collared product. This collared product, which concentration is proportional to the lactates concentration in the sample, is measured spectrophotometrically, according to the fabricants' instructions.

11.2.9 Transepithelial Studies

Confluent BeWo cells were used for permeability studies. Cell monolayer integrity and confluence was assessed by measurement of transepithelial resistance (TEER) before the beginning of each experiment, by using an epithelial voltimeter fitted with planar electrodes (EVOM; World Precision Instruments, Stevenage, UK). Experiments were conducted only in those cell monolayers that showed a TEER >100 Ω, after correction for the resistance obtained in a Snapwell without cells. TEER was also determined after each experiment to determine the effect of test substances on monolayer integrity.

Initially, the culture medium was aspirated and the cells were washed with buffer at 37°C; then the cell monolayers were pre-incubated for 20 min in buffer at 37°C in the absence or presence of tBOOH 100 μM. Uptake was initiated by the addition of 0.3 ml buffer at 37°C containing 20 nM ^{3}H-DG at the apical side, in the absence or presence of tBOOH μM. Samples from the basolateral side were collected every 30 min and incubation was stopped after 120 min, by removing the incubation medium and rinsing the apical side with 0.5 ml ice-cold buffer and the basolateral side with 1.5 ml ice-cold buffer. The cells were then solubilized with 0.3 ml 0.1% (v/v) Triton X-100 in the apical side and with 0.5 ml in the basolateral side, and placed at 4°C overnight. Radioactivity in the cells was measured by liquid scintillation counting and results were expressed as apparent permeability (*P*app).

11.2.10 Calculation and statistics

For the analysis of the time course of ^{3}H-DG uptake, the parameters of Equation 1 were fitted to the experimental data by a non-linear regression analysis, using a computer-assisted method [69].

$$A(t) = k_{in} / k_{out}(1 - e^{-k_{out} \times t}) \qquad (1)$$

A(t) represents the accumulation of ^{3}H-DG at time, k_{in} and k_{out} are the rate constants for inward and outward transport, respectively, and t is the incubation time. A_{max} corresponds to the accumulation (A(t)) at steady state ($t \rightarrow \infty$). k_{in} is given in nmol per milligram protein per

min and k_{out} in min^{-1}. In order to obtain clearance values, k_{in} was converted to µl per milligram protein per min.

For the analysis of the saturation curve of ^{3}H-DG uptake, the parameters of the Michaelis-Menten equation were fitted to the experimental data.

Arithmetic means are given with SEM, and geometric means are given with 95% confidence limits. Statistical analysis of the difference between various groups was evaluated by the ANOVA test, followed by the Student-Newman-Keuls test. Statistical analysis of the difference between two groups was evaluated with Student's t test. Differences were considered to be significant when $P<0.05$.

Papp values were determined according to Equation 2

$$Papp = dQ/dt \cdot 1/ (A \cdot Ci)\ cm/s \quad (2)$$

where dQ/dt (moles per second) is the transport rate, Ci (moles per cubic centimeter) is the initial concentration in the donor chamber, and *A* (square centimeters) is the surface area. Arithmetic means are given with SEM, and geometric means are given with 95% confidence limits. Statistical analysis of the difference between various groups was evaluated by the ANOVA test, followed by the Student-Newman-Keuls test. Statistical analysis of the difference between two groups was evaluated with Student's t test. Differences were considered to be significant when $P<0.05$.

12 Results

12.1 Effect of tBOOH on cell integrity and oxidative stress biomarkers

The first step was to determine the proper concentration of tBOOH to use for inducing oxidative stress in BeWo cells, since our aim was to induce oxidative stress without compromising cell integrity. For that, BeWo cells were submitted to a 24h-treatment to increasing concentrations of tBOOH (1, 3, 10, 30, 100, 300 and 1000 μM), and the cell integrity, as well as some oxidative stress biomarkers, were evaluated.

12.1.1 Cell integrity

In order to assess cell integrity, the effect of tBOOH upon cellular viability and proliferation was evaluated. Exposure of BeWo cells to tBOOH 300 μM and 1000 μM caused an increase in LDH leakage, indicating that these concentrations did affect cell membrane integrity (Fig. 12 left side). Similarly, treatment with tBOOH 300 μM and 1000 μM caused a significant decrease in BeWo cell proliferation (Fig.12 right side).

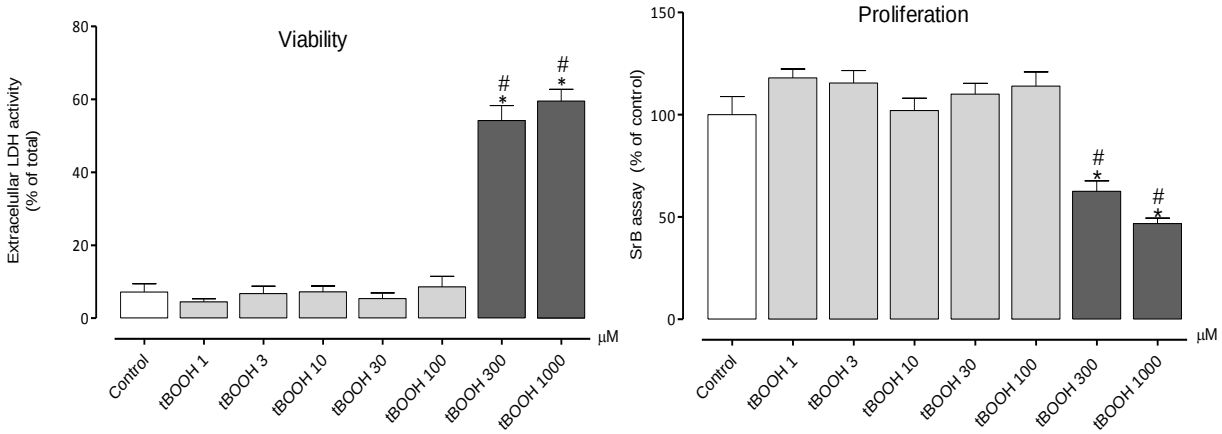

Figure 12: Effect of tBOOH on cell viability (left panel) and cell proliferation (right panel). After a 24h-exposure to different concentrations of tBOOH (1-3000 μM) or its solvent (control), BeWo cellular viability was determined by quantification of extracellular LDH activity (n=9-12) and cellular proliferation was determined by quantification of whole cellular protein with SRB (n=9-12). Shown are arithmetic means ±S.E.M. *significantly different from control ($P < 0.05$). #significantly different from tBOOH 1-100 μM

Considering these results, some important biomarkers were then analyzed for tBOOH 10, 30 and 100 μM, in order to evaluate oxidative stress levels.

12.1.2 Oxidative stress biomarkers

12.1.2.1 Glutathiones

One of the biomarkers analysed were the cellular levels of total (GSx), oxidized (GSSG) and reduced (GSH) glutathione, as well as the GSH/GSSG ratio.

BeWo cells were treated with tBOOH 10, 30 and 100 µM for 24h, and the results are presented in Fig. 13. As shown, levels of total glutathione (GSx) were significantly increased with tBOOH 30 and 100 µM. Moreover, levels of oxidized glutathione (GSSG) were increased with tBOOH 100 µM. As for reduced glutathione (GSH) levels, no significant changes were observed.

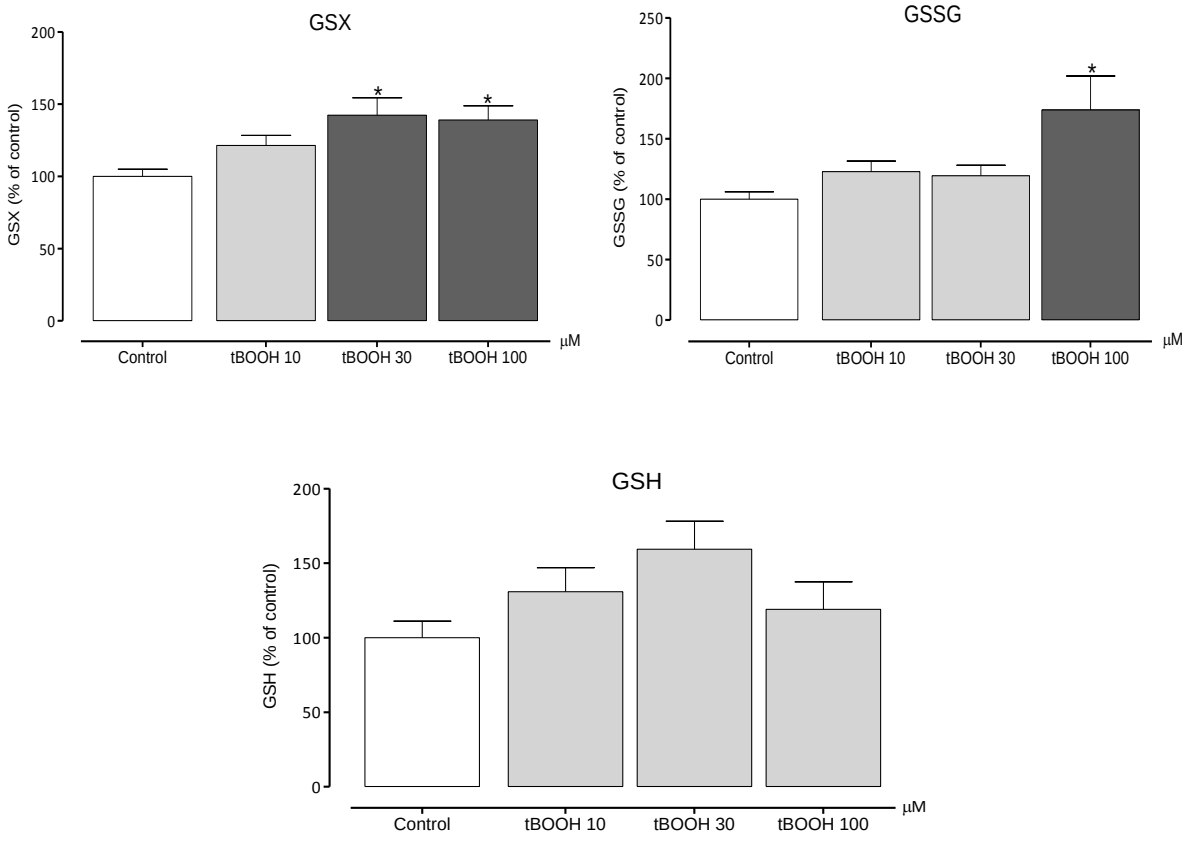

Figure 13: Effect of tBOOH on total (GSx), oxidized (GSSS) and reduced (GSH) glutathione levels. These parameters were determined after a 24h-exposure of BeWo cells to concentrations of tBOOH (10-100 µM) that did not affect neither cellular viability nor proliferation or to the respective solvent (control) (n=9-16). Shown are arithmetic means ±SEM. *significantly different from control ($P < 0.05$).

To further evaluate the effect of tBOOH upon oxidative stress levels, two other two biomarkers were also assessed.

12.1.2.2 Lipidic peroxidation and carbonylated proteins

The extent of lipid peroxidation was measured by using the TBARS assay. Lipid peroxidation results in the formation of reactive aldehydes, including malondialdehyde (MDA). The extent of protein carbonylation was evaluated by measuring protein carbonyl groups, which are produced on protein side chains when they are oxidized. tBOOH 100 µM caused a significant increase in MDA levels, indicating oxidative damage to cell lipids (Fig. 14, left side) and a significant increase in the concentration of carbonyl groups, indicating oxidative damage to proteins (Fig. 14, right side).

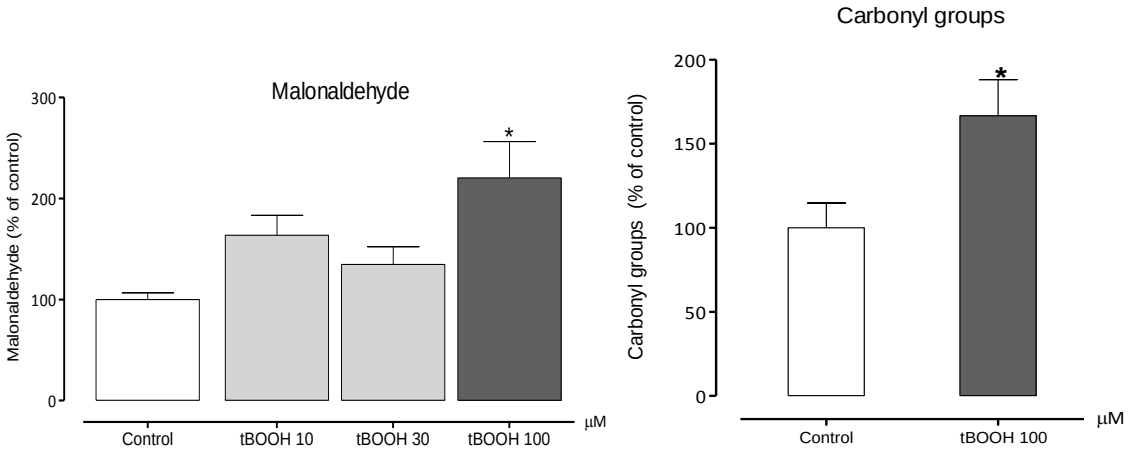

Figure 14: Effect of tBOOH on MDA (lipid peroxidation product) and protein carbonyl levels in BeWo cells. These parameters were determined after a 24h-exposure of BeWo cells to concentrations of tBOOH (10-100 µM) that did not affect neither cellular viability nor proliferation or to the respective solvent (control) (n=15-30). Shown are arithmetic means ±SEM. *significantly different from control ($P < 0.05$).

12.2 Effect of tBOOH on ^{3}H-2-D-glucose uptake

12.2.1 Effect of tBOOH on total uptake

In a first series of experiments, the time-course of ^{3}H-DG (50 nM) accumulation in BeWo cells was determined. For this, cells were incubated at 37°C with ^{3}H-DG for various periods of time,

(1, 5, 10, 30, 90 and 120 min), in the absence or presence of a previous treatment with 100 µM tBOOH for 24h. As shown in Fig. 15, treatment with tBOOH originated a reduced accumulation of ^{3}H-DG over time. Analysis of the time-course of ^{3}H-DG accumulation showed a decrease of about 33% in the A_{max} in the presence of tBOOH. Also, both the k_{in} and k_{out} were significantly different between control and tBOOH (Table 3). Analysis of Table 3 shows that, in control conditions, an amount of cells corresponding to 1 mg of cell proteins removed the ^{3}H-DG present in 9.5 µL of buffer and that, simultaneously, 3% of intracellular ^{3}H-DG left the cells per min. On the other hand, after treatment with tBOOH, an amount of cells corresponding to 1 mg removed the ^{3}H-DG present in 16.1 µL of buffer and, simultaneously, 8% of intracellular ^{3}H-DG left the cells per minute.

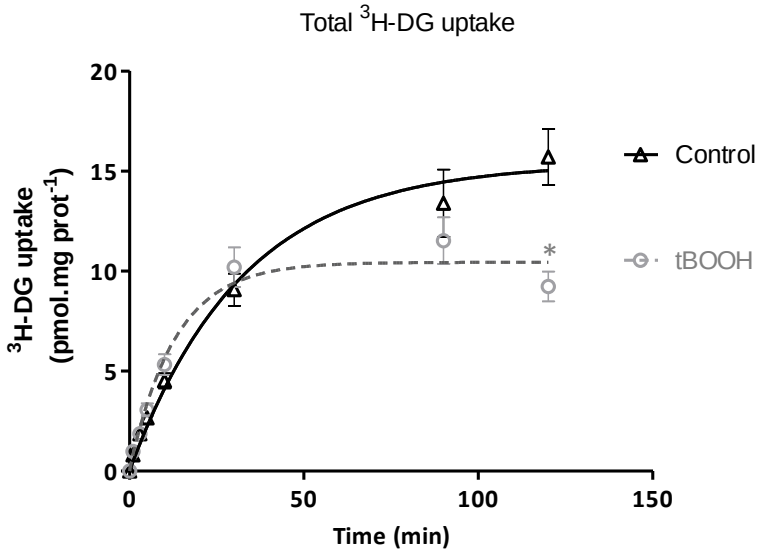

Figure 15: Effect of tBOOH upon the time-course of 3H-DG apical uptake by BeWo cells. Cells were exposed for 24h to tBOOH 100 µM or the respective solvent (control). After that, cells were incubated in buffer with Na+ at pH 7.4, containing 50 nM ^{3}H-DG, for various periods of time (n=6-17). Shown are arithmetic means ±S.E.M. *significantly different from control ($P < 0.05$).

Table 3: Analysis of the time course of 3H-DG apical uptake by BeWo cells. Cells were exposed for 24h to tBOOH 100 µM or the respective solvent (control). Analysis allowed determination of the steady state of accumulation (Amax) and the rate constant for inward (k_{in}) and outward (k_{out}) transport. Shown are arithmetic means ±S.E.M. *significantly different from control ($P < 0.05$).

	A_{max} (pmol.mg prot^{-1})	K_{in} (µL.mg prot^{-1}.min^{-1})	K_{out} (min^{-1})
Control	15.4 ± 0.9	9.5 ± 1.5	0.03 ± 0.006
tBOOH	10.4 ± 0.5*	16.1 ± 2.2*	0.08 ± 0.01*

12.2.2 Effect of tBOOH on GLUT-dependent and GLUT-independent uptake

At this point, it was important to characterize ^{3}H-DG uptake in BeWo cells in both, normal conditions (control) and under oxidative stress conditions (tBOOH), by investigating how much of ^{3}H-DG uptake was GLUT-mediated. In order to do so, a GLUT inhibitor (cytochalasin B 50 µM) was used. This compound was already used by the group to inhibit GLUT activity in the BeWo cell line. [27] The results show that cytochalasin B 50 µM inhibits about 50% of ^{3}H-DG uptake (Fig. 16). Also, both the k_{in} and k_{out} were significantly different between control and cytochalasin B (Table 4). Indeed, analysis of Table 4 shows that, in control conditions, an amount of cells corresponding to 1 mg of cell proteins removed the ^{3}H-DG present in 9.5 µL of buffer and that, simultaneously, 3% of intracellular ^{3}H-DG left the cells per min. On the other hand, after treatment with cytochalasin B, an amount of cells corresponding to 1 mg removed the ^{3}H-DG present in 2.37 µL of buffer and, simultaneously, 1.6% of intracellular ^{3}H-DG left the cells per minute.

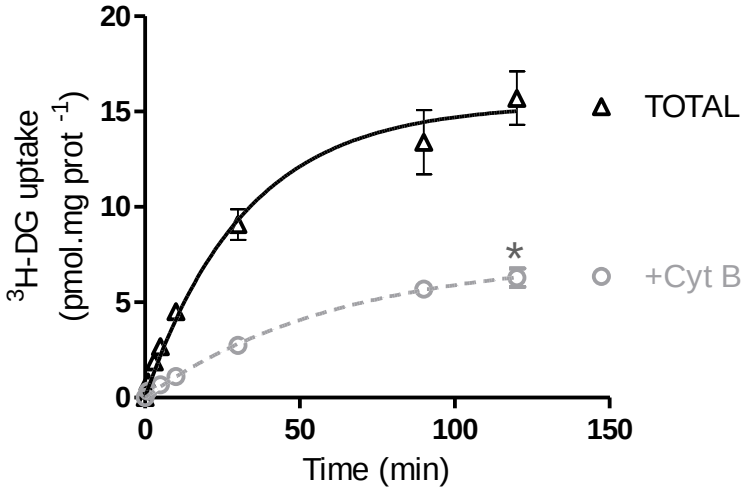

Figure 16: Time-course of 3H-DG uptake by BeWo cells. Cells were incubated in buffer with Na+ (TOTAL, black curve) or in buffer without Na+ and in the presence of cytochalasin B 50 µM (Cyt B (non-GLUT mediated); grey curve) at pH 7.4, containing 50 nM ^{3}H-DG, for various periods of time (n=6-17). *significantly different from control ($P < 0.05$).

Table 4: Analysis of the time course of 3H-DG apical uptake by BeWo cells. Cells were incubated in buffer with Na+ (control) or in buffer without Na+ and in the presence of cytochalasin B 50 µM (Cyt. B). Analysis allowed determination of the steady state accumulation (A_{max}) and the rate constant for inward (k_{in}) and outward (k_{out}) transport. Shown are arithmetic means ±SEM. *significantly different from control (P < 0.05)

	A_{max} (pmol.mg prot^{-1})	k_{in} (µL.mg prot^{-1}.min^{-1})	k_{out} (min^{-1})
Control	15.40 ± 0.90	9.5 ± 1.5	0.031 ± 0.006
Cyt. B	7.39 ± 0.82*	2.37 ± 0.38*	0.016 ± 0.004*

Another commonly used GLUT inhibitor, phloretin (2 mM), was also simultaneously tested as a possibly more appropriate and effective GLUT inhibitor.

The results, presented in Fig. 17, show that phloretin (2 mM) inhibited ^{3}H-DG uptake more markedly than cytochalasin B (80% vs. 50% inhibition, respectively). However, phloretin (2 mM) compromises cell viability (it caused a significant increase of extracellular LDH activity) and significantly decreases cell proliferation (Fig. 18).

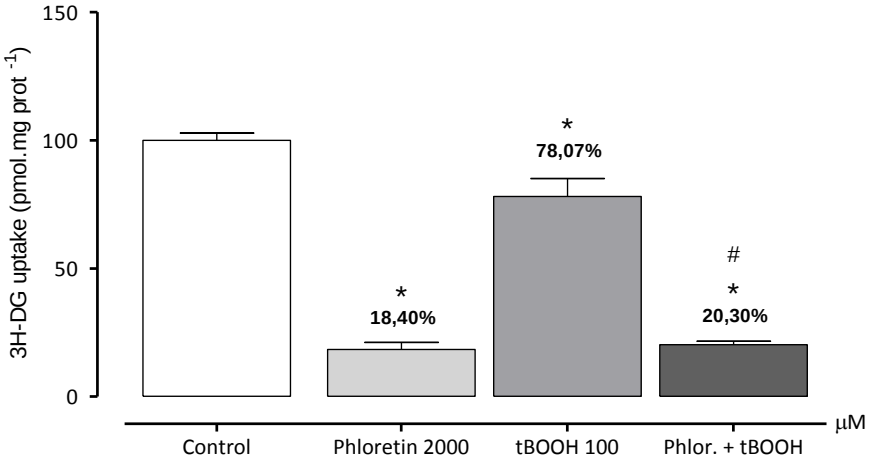

Figure 17: ^{3}H-DG uptake by BeWo cells. Cells were exposed for 24h to tBOOH 100 µM or the respective solvent (control). After that, cells were incubated in buffer in the absence (control) or presence of phloretin (2 mM). *Significantly different from control (P < 0.05). #significantly different from tBOOH 100 µM.

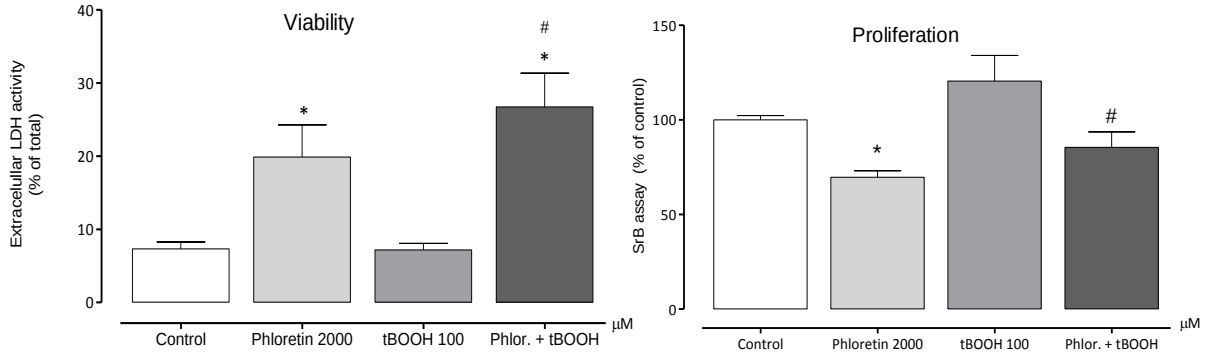

Figure 18: Effect of phloretin (2 mM) and tBOOH (100 µM) on cell viability (left panel) and cell proliferation (right panel). After a 24h-exposure of tBOOH 100 µM or its solvent (control), BeWo cellular viability was determined by quantification of extracellular LDH activity (n=6) and cellular proliferation was determined by quantification of whole cellular protein with SRB (n=6).*significantly different from control ($P < 0.05$). #significantly different from tBOOH 100 µM

Contrary to phloretin, cytochalasin B´s effect on ^{3}H-DG uptake was not related to a decrease in cell proliferation or viability (Fig. 19). So, cytochalasin B was chosen as the GLUT1 inhibitor in the next series of experiments.

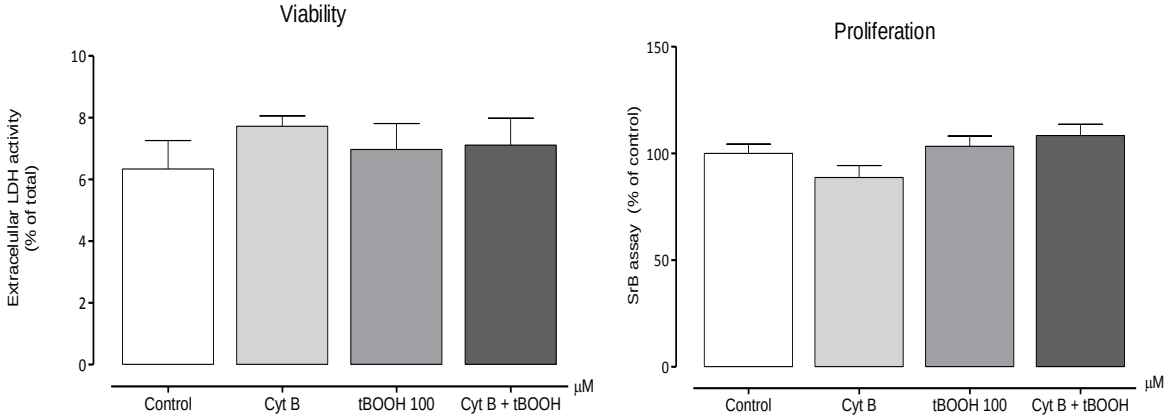

Figure 19: Effect of cytochalasin B (50 mM) and tBOOH (100 µM) on cell viability (left panel) and cell proliferation (right panel). After a 24h-exposure of tBOOH 100 µM or its solvent (control), BeWo cellular viability was determined by quantification of extracellular LDH activity (n=6) and cellular proliferation was determined by quantification of whole cellular protein with SRB (n=6).

In the next series of experiments, the time-course of ^{3}H-DG uptake under control and oxidative stress conditions was analysed in the absence and presence of cytochalasin B 50 µM. For that, cells were incubated at 37°C with ^{3}H-DG for various periods of time (1, 5, 10, 30, 90 and 120 min), in the absence or presence of a previous treatment with 100 µM tBOOH for 24h. After that, cells were incubated in buffer with Na^{+} (total uptake) or in Na^{+}-free buffer containing cytochalasin B 50 µM (non-GLUT-mediated uptake). GLUT-mediated uptake was obtained by subtracting non-GLUT-mediated uptake from total uptake. The results obtained show that tBOOH reduces both GLUT-mediated and non-GLUT-mediated ^{3}H-DG uptake (Fig. 20 and 21) as well as the A_{max} for GLUT-mediated and non-GLUT-mediated (Tables 5 and 6, respectively).

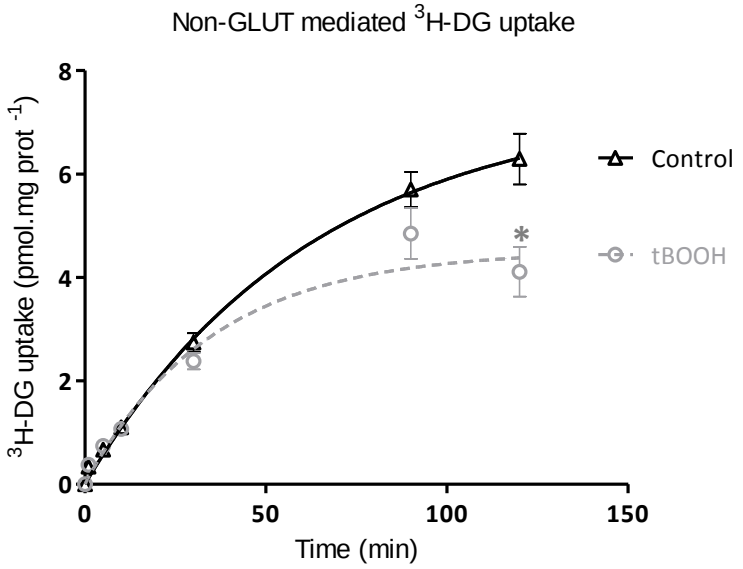

Figure 20: Time-course of non-GLUT-mediated ^{3}H-DG uptake, by BeWo cells. Cells were exposed for 24h to tBOOH 100 µM or the respective solvent (control). After that, cells were incubated in Na+-free buffer in the presence of cytochalasin B 50 µM (non-GLUT-mediated uptake), containing 50 nM ^{3}H-DG, for various periods of time (n=6-17).

Table 5: Analysis of the time course allowed determination of the steady state accumulation (A_{max}) and the rate constant for inward (k_{in}) and outward (k_{out}) transport. Shown are arithmetic means ±SEM. *significantly different from control ($P < 0.05$).

	A_{max} (pmol.mg prot^{-1})	**k_{in} (µL.mg prot^{-1}.min^{-1})**	**k_{out} (min^{-1})**
Control	7.4 ± 0.8	2.366 ± 0.383	0.016 ± 0.004
tBOOH	4.5 ± 0.3*	2.600 ± 0.556	0.029 ± 0.007

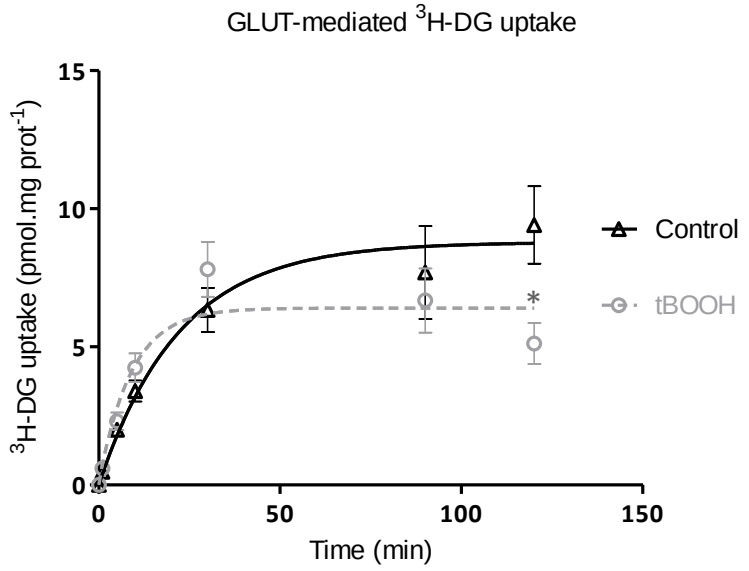

Figure 21: Time-course of GLUT-mediated ^{3}H-DG uptake, by BeWo cells. Cells were exposed for 24h to tBOOH 100 µM or the respective solvent (control). After that, cells were incubated in Na^{+}-containing buffer (total uptake) or in Na^{+}-free buffer in the presence of cytochalasin B 50 µM (non-GLUT-mediated uptake), containing 50 nM ^{3}H-DG, for various periods of time (*n*=6-18). GLUT-mediated uptake was obtained by subtracting non-GLUT-mediated uptake from total uptake. Shown are arithmetic means ±SEM. *significantly different from control ($P < 0.05$).

Table 6: Analysis of the time course of GLUT-mediated ^{3}H-DG uptake allowed determination of the steady state accumulation (A_{max}) and the rate constant for inward (k_{in}) and outward (k_{out}) transport. (Table above) Shown are arithmetic means ±SEM. *significantly different from control ($P < 0.05$).

	A_{max} (pmol.mg prot^{-1})	k_{in} (µL.mg prot^{-1}.min^{-1})	k_{out} (min^{-1})
Control	8.8 ± 0.7	7.9 ± 2.1	0.05 ± 0.01
tBOOH	6.4 ± 0.5*	14.5 ± 3.5	0.10 ± 0.03

12.2.3 Effect of tBOOH upon GLUT1 mRNA levels

Next, mRNA levels of GLUT1 were quantified, by qRT-PCR, in order to verify if tBOOH changes GLUT1 gene expression.

Table 7: Results concerning GLUT1's mRNA expression after a 24h-treatment of BeWo cells with tBOOH 100 µM or the respective solvent (control). HPRT is the housekeeping gene (hypoxanthine-guanine phosphoribosyltransferase).

(GLUT1/HPRT)	Mean	SEM	n
Control	0.15990	0.03312	5
tBOOH	0.10494	0.02840	4

The results, shown in Table 7, lead to the conclusion that the expression of GLUT1 is not significantly altered in response to oxidative stress induced by tBOOH.

12.2.4 Effect of tBOOH upon lactate production

Considering that cellular cultures perform mainly anaerobic glycolysis, we investigated if the decrease in glucose cellular uptake in response to tBOOH exposure, as assessed by the decrease in ^{3}H-DG uptake, would cause also a decrease in anaerobic respiration rates. For that, we quantified lactate levels in both situations.

Table 8: Quantification of lactate (mmol.mg prot^{-1}) in cells exposed for 24h to tBOOH 100 µM or to the respective solvent (control). Results are presented as arithmetic means ±SEM.

Lactate	Mean	SEM	n
Control	27.730	0,736	17
tBOOH	29.665	1.340	17

The results demonstrate no significant difference between the amount of lactate present in cultures under normal and oxidative stress conditions (Table 8).

12.2.5 Involvement of PI3K and PKC on the effect of tBOOH

In the next series of experiments, we evaluated if two intracellular pathways, phosphatidylinositol 3-kinases (PI3K) and protein kinase C (PKC), that are activated during oxidative stress stimuli [70], and that can alter cellular glucose uptake [71, 72], were compromised by tBOOH.

Chelerythrine 0.1 µM was used as an inhibitor of PKC pathway and LY 294002 1 µM was used as an inhibitor of PI3K/Akt pathway.

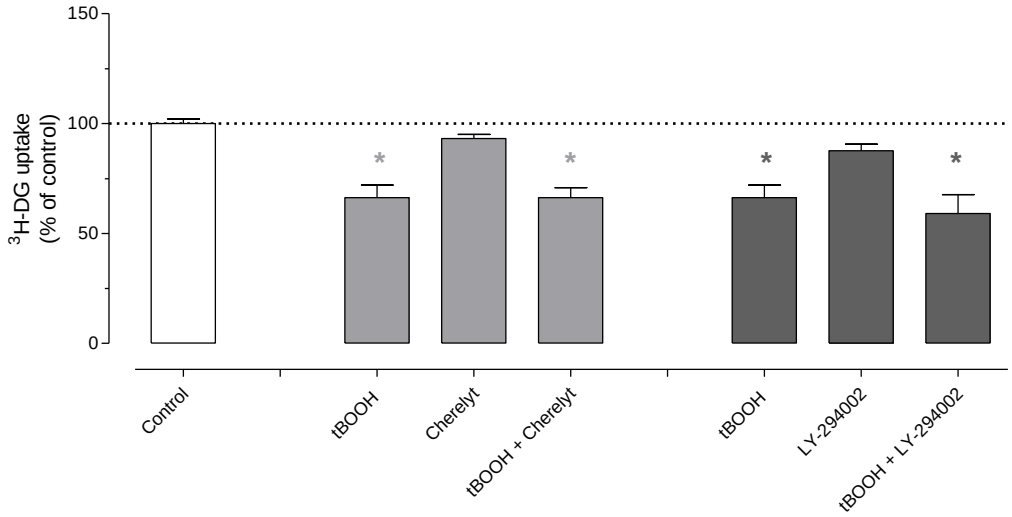

Figure 22: Influence of PI3K/Akt and PKC pathways (n=9-12) upon the decrease of ^{3}H-DG uptake caused by a 24h-exposure of BeWo cells to tBOOH (100 µM). Shown are arithmetic means ±SEM. *significantly different from control (total) ($P < 0.05$).

The results concerning the influence of chelerythrine and LY 294002 show that neither of these compounds affected ^{3}H-DG total uptake, whether in control conditions or in the presence of tBOOH (Fig. 22).

12.2.6 Effect of some antioxidants

Next, we decided to investigate in the observed effect of oxidative stress upon ^{3}H-DG uptake could be reverted by antioxidants.

First, two inhibitors of ROS producing enzymes were analyzed: apocynin (1mM), an inhibitor of NADPH-oxidase, and allopurinol (1 mM), an inhibitor of xanthine oxidase.

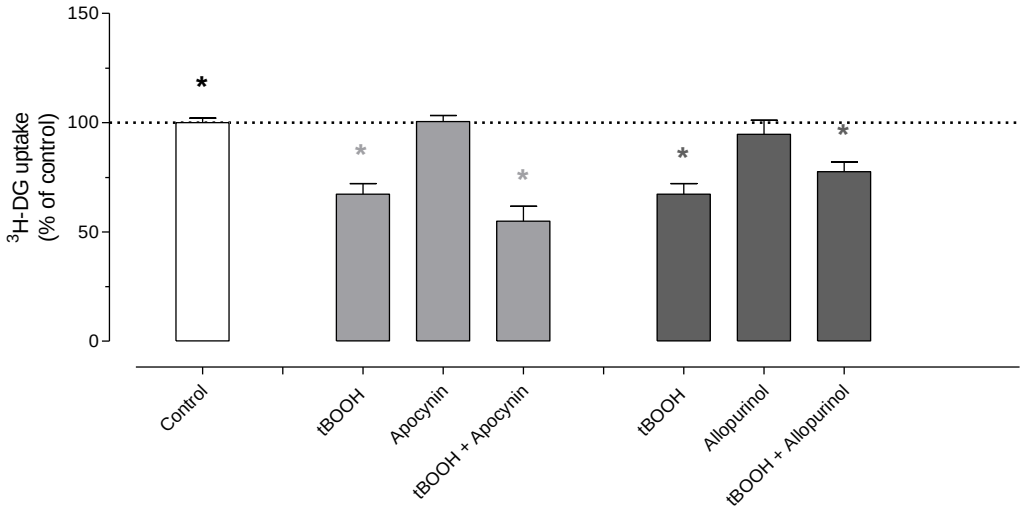

Influence of NADPH oxidase (apocynin 1mM) and xanthine oxidase (allopurinol 1mM) inhibitors (n=9) upon the decrease of ^{3}H-DG uptake caused by a 24h-exposure of BeWo cells to tBOOH (100 µM). Shown are arithmetic means ±SEM. *significantly different from control (total) ($P < 0.05$).

Results in Fig.23 show that none of the enzymes seem to be affecting ^{3}H-DG uptake by cells, because their inhibition had no effect upon it. Moreover, inhibition of these enzymes, responsible for the production of ROS, also did not alter the effect of tBOOH.

Then, some diet antioxidants were tested.

Vitamin E (α-tocopherol 1 mM) showed no significant reversion of tBOOH's effect upon ^{3}H-DG uptake (Fig.24). Similar results, shown in Fig.25, were found for N-acetylcysteine (NAC) 0.1 mM.

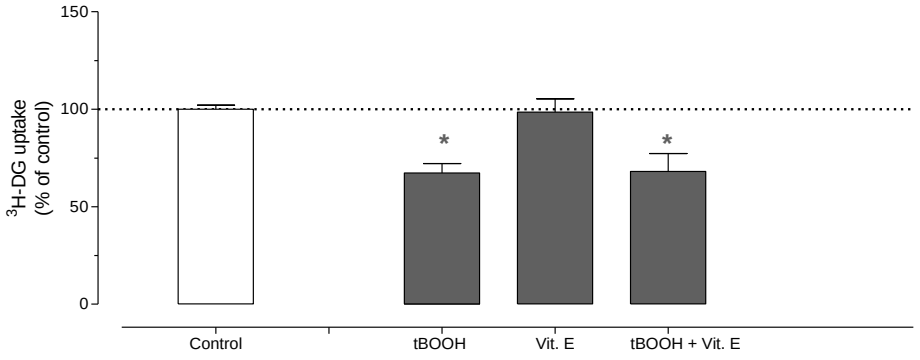

Figure 23: Influence of vitamin E 1 mM (n=9) upon the decrease of ^{3}H-DG uptake caused by a 24h-exposure of BeWo cells to tBOOH (100 µM). Shown are arithmetic means ±SEM. *significantly different from control (total) ($P < 0.05$).

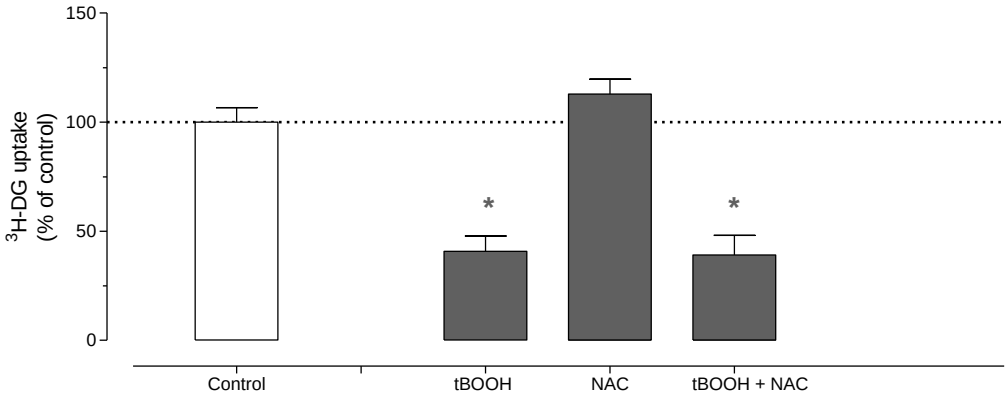

Figure 24: Influence of NAC 1 mM (n=9) upon the decrease of ^{3}H-DG uptake caused by a 24h-exposure of BeWo cells to tBOOH (100 µM). Shown are arithmetic means ±SEM.*significantly different from control (total). ($P < 0.05$)

Finally, we tested some diet polyphenols. Interestingly, resveratrol 50 µM (Fig.25), quercetin 50 µM (Fig.26) and EGCG 50 µM (Fig.27), presented similar effects. For the three polyphenols, the polyphenol by itself did not shown a significant difference from the respective control but, together with tBOOH, a significant, although not complete, reversion of the oxidative stress effect of tBOOH on ^{3}H-DG uptake was found.

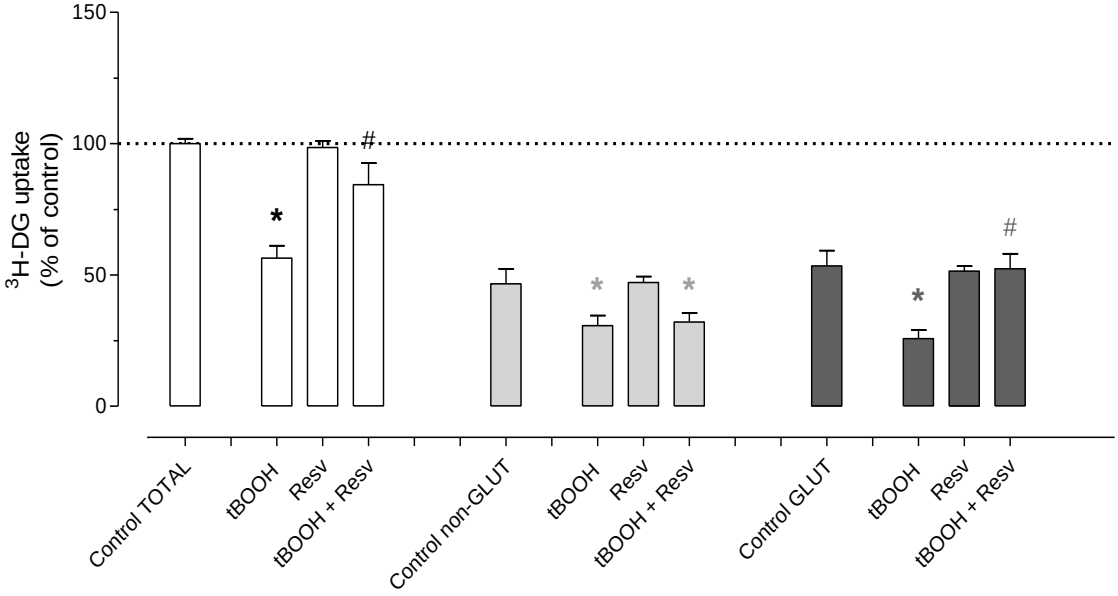

Figure 25: Influence of resveratrol 50 µM (n=12) upon the decrease of ^{3}H-DG uptake caused by a 24h-exposure of BeWo cells to tBOOH (100 µM). Shown are arithmetic means ±SEM.*significantly different from control (total). $^{\#}$significantly different from tBOOH 100 µM ($P < 0.05$)

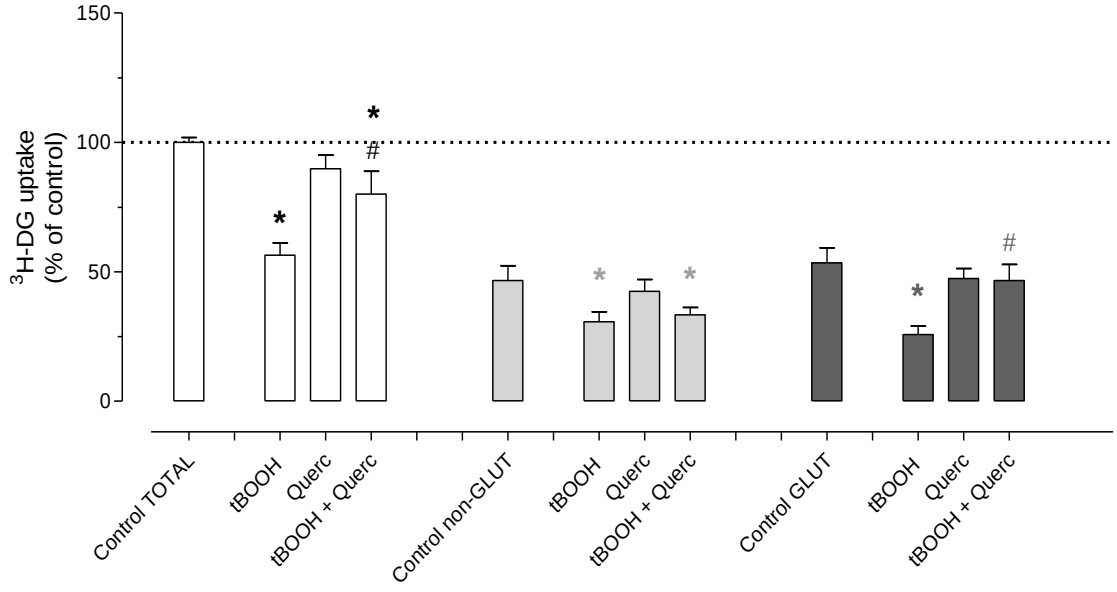

Figure 26: Influence of quercetin 50 µM (n=12) upon the decrease of ^{3}H-DG uptake caused by a 24h-exposure of BeWo cells to tBOOH (100 µM). Shown are arithmetic means ±SEM. *significantly different from control (total). #significantly different from tBOOH 100 µM ($P < 0.05$)

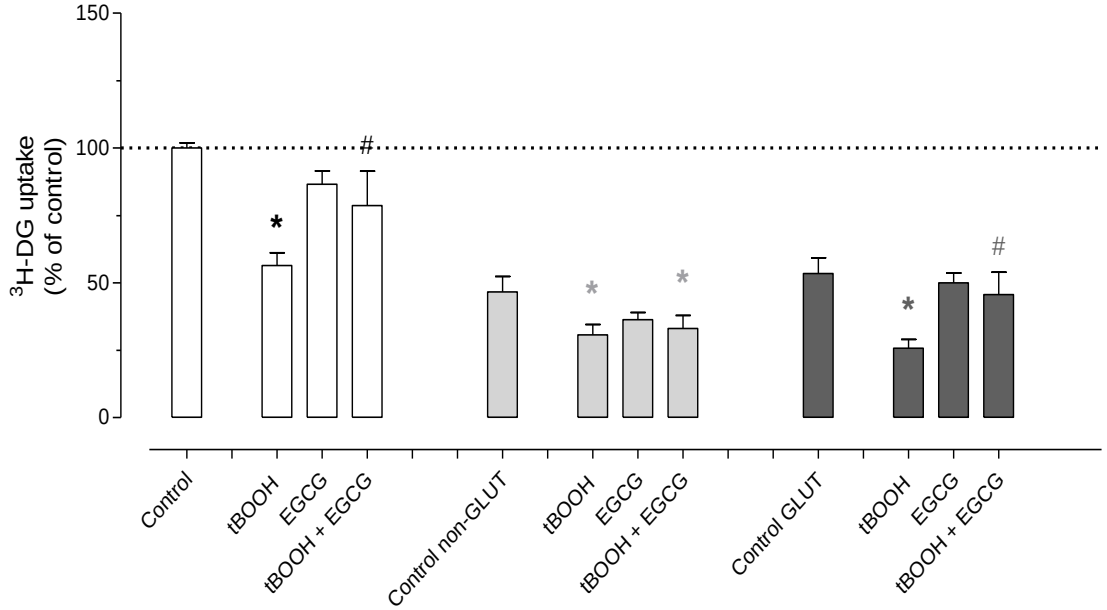

Figure 27: Influence of EGCG 50 µM (n=12) upon the decrease of ^{3}H-DG uptake caused by a 24h-exposure of BeWo cells to tBOOH (100 µM). Shown are arithmetic means ±SEM. *significantly different from control (total). #significantly different from tBOOH 100 µM ($P < 0.05$)

In Table 9, at bold, are presented the results that are significantly different, considering GLUT-mediated and non-GLUT mediated ^{3}H-DG uptake, separately. The same kind of results is presented for quercetin (Table 10) and for EGCG (Table 11).

Table 9: Results of ^{3}H-DG uptake regarding resveratrol.

	Uptake (% of control)		
	TOTAL	Non-GLUT mediated	GLUT mediated
Control	100.00 ± 1.90	46.58 ± 5.79	53.42 ± 5.85
Resveratrol	98.64 ± 2.57	**47. 10 ± 2.27**	51.43 ±1.91
tBOOH	56.42 ± 4.70	30.68 ±3.88	**25.74 ± 3.29**
tBOOH + Resveratrol	84.42 ± 8.20	**32.08 ± 3.50**	**52.34 ± 5.73**

Table 10: Results of ^{3}H-DG uptake regarding quercetin.

	Uptake (% of control)		
	TOTAL	Non-GLUT mediated	GLUT mediated
Control	100.00 ± 1.90	46.58 ± 5.79	53.42 ± 5.85
Quercetin	89.85 ± 5.27	**42. 46 ± 4.58**	47.39 ± 3.87
tBOOH	56.42 ± 4.70	30.68 ±3.88	**25.74 ± 3.29**
tBOOH + Quercetin	80.00 ± 8.82	**33.33 ± 2.93**	**46.67 ± 6.17**

Table 11: Results of ^{3}H-DG uptake regarding epigallocatechin-3-gallate.

	Uptake (% of control)		
	TOTAL	Non-GLUT mediated	GLUT mediated
Control	100.00 ± 1.90	46.58 ± 5.79	53.42 ± 5.85
EGCG	86.61 ± 4.91	**36.38 ± 2.59**	49.96 ± 3.71
tBOOH	56.42 ± 4.70	30.68 ±3.88	**25.74 ± 3.29**
tBOOH + EGCG	78.64 ± 12.82	**33.04 ± 4.88**	**45.61 ± 8.32**

12.3 Effect of tBOOH on the transcellular transport of ^{3}H-DG

Fig. 28 represents the results regarding the ^{3}H-DG transepithelial transport across BeWo cells. The graphic shows the apical-to-basolateral transepithelial transport of ^{3}H-DG uptake with time, while the inset (up on the left of the graphic) shows the apical ^{3}H-DG uptake, at 120 min.

Concerning the apical uptake, the results are in agreement with the already presented (section 7.2.1. - Effect of tBOOH on total uptake), showing a significant decrease in ^{3}H-DG apical cellular uptake.

Results concerning the apical-to-basolateral transport show that ^{3}H-DG transepithelial transport increases with time, in a linear manner, both in the absence and presence of tBOOH. Moreover, in the presence of tBOOH, apical-to-basolateral ^{3}H-DG transport is higher than control (Fig. 28).

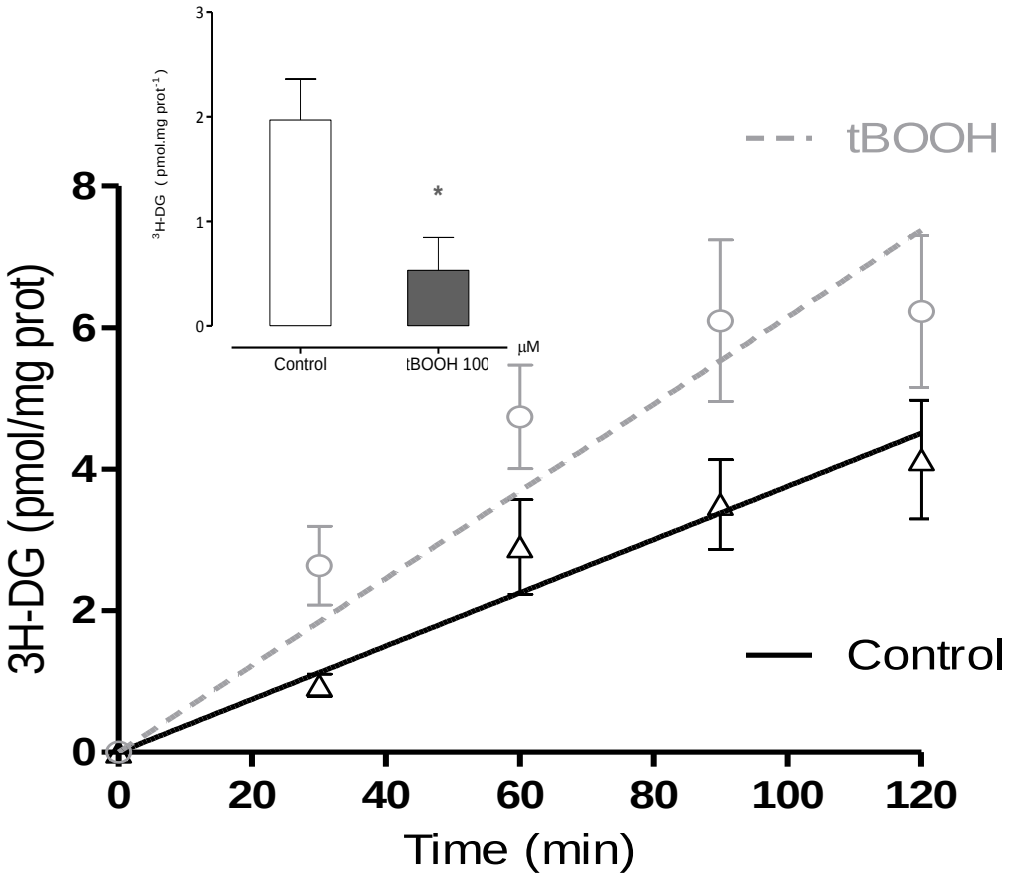

Figure 28: Apical-to-basolateral transepithelial transport of ^{3}H-DG, in normal conditions (control) and under oxidative stress (tBOOH) (n=6). The inset represents the ^{3}H-DG apical cellular uptake.*significantly different from respective control. ($P < 0.05$)

The P_{app} (apparent permeability) was calculated in the absence and presence of tBOOH and results are presented in Table 12. The mean value, for an n of 6, of control was 1,676 x 10^{-03} ± 1,057 x 10^{-04} cm/s, while for tBOOH was 2,743 x 10^{-03} ± 2,494 x 10^{-04} cm/s. So, tBOOH causes an increase in P_{app} of ^{3}H-DG in the apical-to-basolateral direction.

Table 12: Apical-to-basolateral apparent permeability (Papp) to ^{3}H-DG across BeWo cells in normal conditions (control) and under oxidative stress (tBOOH). *significantly different from respective control. (P < 0.05)

Papp (cm/s)	Mean	SEM	n
Control	1,676 x 10^{-03}	1,057 x 10^{-04}	6
tBOOH	2,743 x 10^{-03} *	2,494 x 10^{-04} *	6

13 Discussion

Based on previous studies, tBOOH was chosen as an inducer of oxidative stress in the BeWo trophoblastic cell line, BeWo [35, 63, 64]. From tBOOH, tested at 1, 3, 10, 30, 100, 300 and 1000 μM, the proper concentration was chosen, after the evaluation of cell integrity and important oxidative stress biomarkers. Based on the assays of cell viability (LDH leakage) and cell proliferation (SRB assay), we concluded that cell integrity is compromised for the two highest concentrations of tBOOH (300 and 1000 μM).

Taking these results into consideration, the evaluation of the following oxidative stress biomarkers was conducted for tBOOH 10, 30, 100 μM: glutathiones, lipid peroxidation and carbonylated proteins.

Glutathiones (GSH) are thiol-containing tripeptides (γ-glutamyl-cysteinyl-glycine) that have a major role in cellular protection against the toxicity induced by oxidant agents. Several studies show that GSH possesses a number of important functions implicated in cell physiology and pathophysiology, such as DNA synthesis and cell proliferation, regulation of nuclear matrix organization and maintenance of Cys residues on zinc-finger DNA-binding motifs in a reduced and functional state [73]. The millimolar levels of cellular GSH (5-10 mM) are distributed mainly between the cytosolic (about 80-85%) and mitochondrial (10-15%) compartments and the ratio $[GSH]^2/[GSSG]$ determines the cellular redox state, with GSH representing the reduced form and GSSG the oxidized form [46, 73]. ROS glutathione peroxidase (GPx) catalyzes the reduction of H_2O_2 or organic hydroperoxides to H_2O and respective alcohols by using GSH as a reductant. Simultaneously, the Cys residues of GSH are oxidized forming disulfides (S-glutathionylation), so it is expected that increased levels of oxidative stress implicate a lower $[GSH]^2/[GSSG]$ ratio [33, 74]. Using colorimetric and enzymatic assays it was possible to quantify these two forms, by calculating their levels through the reaction GSx = GSH + 2 GSSG, with GSx being total glutathione [75].

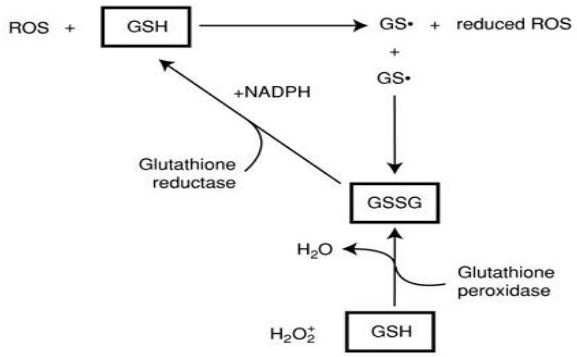

Figure 29: Interconversion of glutathione (GSH) and GSSG in the presence of reactive oxygen species (ROS), which are non-enzymatically reduced by GSH. [1]

Glutathiones levels were assessed for the three highest tBOOH concentrations that did not compromise cell integrity (10, 30 and 100 μM). It was concluded that total glutathione levels (GSx) were significantly increased for tBOOH 30 and 100 μM and that GSSG levels were significantly increased for tBOOH 100 μM. Since the ratio $[GSH]^2/[GSSG]$ decreases as oxidative stress levels increase (as already mentioned in Introduction), these results indicate that tBOOH 100 μM would be the proper concentration to induce oxidative stress on cells without compromising its integrity.

Nevertheless, lipid peroxidation, as well as carbonylated proteins, was measured.

Lipid peroxidation is a process that depends on the presence of free radicals and is involved in the modification of membrane structure and permeability, age pigment formation, oxidative modification of low-density lipoproteins and alteration of vasomotor tone regulation [63].

Mammalian cells contain 1500-2000 lipid species. [76] Unsaturated lipids have methylene (-CH_2) groups, where hydrogens are particularly reactive. ROS have the ability to scavenge electrons from these groups, forming a lipid radical, which then can react with oxygen and other fatty acids to produce lipid hydroperoxides. It is a chain reaction that can significantly alter the membranes' fluidity, permeability transport and metabolic processes. Fatty acid peroxides can give rise to various aldehydes with proven toxicity, such as like 4-hydroxy-2-nonenal, that causes extensive damage and results in apoptosis. There are also aldehydes, mainly α,β-unsaturated reactive aldehydes, resulting from lipid peroxidation and, because they are more stable than ROS, they can serve as "second cytotoxic messengers" and react with proteins' side chains, forming carbonylated proteins, for example (already mentioned above). A good example is malondialdehyde (MDA), a physiologic ketoaldehyde that is produced in excess as a result of tissue injury and reacts mainly with L-Lys residues by Michael addition. Modification of proteins by MDA can alter their biological properties and their immunogenic [33, 76, 77].

Carbonyl (CO) groups, aldehydes and ketones, are chemically stable compounds that result from oxidative stress and, therefore, constitute a reliable way to verify cell damage. In fact, protein carbonyl content is by far the most common used marker of protein oxidation and its accumulation has been related to several human diseases like Alzheimer, diabetes, inflammatory bowel disease and arthritis, naming just a few. For example, analysis of plasma proteins of children with different forms of chronic arthritis showed significantly higher carbonyl levels when compared with healthy children. The same has been observed in

patients with acute pancreatitis, chronic kidney disease and Alzheimer, confirming that this protein modification can be a useful plasma marker of oxidative stress [33, 34]. CO groups have several sources, such as oxidation of aminoacid (namely Pro, Arg, Lys and Thr) side chains, oxidative cleavage of proteins by α-amidation pathway or glutamyl side chains, or even by secondary reaction of a nucleophilic side chain of Cys, His, and Lys residues, with aldehydes, produced during lipid peroxidation, or with reactive carbonyl derivates, generated during sugars' reduction, for example [33, 34].

Although protein CO groups can be induced by almost all ROS' types, not being very conclusive about the source of the oxidative stress, their content evaluation, together with other biomarkers, constitute a solid indicator about the cell's integrity [34].

The results obtained reinforced the previous conclusion, as MDA levels and carbonylated proteins were significantly increased by tBOOH 100 μM. Therefore, tBOOH 100 μM (24 h) was used in all subsequent experiments.

In this work, glucose uptake was studied by using ^{3}H-DG as a substrate. DG is a D-glucose analogue that is efficiently transported by facilitated glucose transporters such as GLUT1 and GLUT2, but is poorly transported by SGLT1 [78]. Moreover, once inside cells, this compound is phosphorylated by hexokinase to 2-deoxy-D-glucose-6-phosphate, which is metabolically inactive and poorly transportable across biological membranes [78]. So, accumulation of ^{3}H-DG-6-phosphate in cells is a good estimate of ^{3}H-DG rates of uptake.

To evaluate if glucose uptake would be altered under oxidative stress condition, a time-course of ^{3}H-DG uptake was conducted. The results showed that tBOOH inhibited ^{3}H-DG uptake in a time-dependent manner, causing a decrease in A_{max} of ^{3}H-DG uptake. Also, analysis of the effect of tBOOH over time showed that its effect upon ^{3}H-DG uptake was maximal at 120 min of incubation. Based on these results, a 120 min incubation time was chosen as the standard incubation for subsequent experiments.

Observation of an inhibitory effect of tBOOH upon ^{3}H-DG uptake originated some questions:

1. Is this effect a result of changes in GLUT activity /transcription rates?
2. Will this inhibitory effect reflect upon intracellular lactate levels?
3. Is this effect dependent on the activation of intracellular signaling pathways?
4. Can the effect be reversed with antioxidants?
5. Will this effect cause a decrease in the transepithelial transport of ^{3}H-DG?

To answer the first question, a GLUT inhibitor, cytochalasin B (50 μM), was used in transport assays. Cytochalasin B is a largely used compound to study the role of GLUT transporters in the uptake of glucose. There have been reports of inhibition from 50% up to 85%, varying according, among other features, the concentration of the inhibitor and glucose [26, 27]. In our experimental conditions, about 50% of ^{3}H-DG uptake by BeWo cells seems to be GLUT-mediated. Under oxidative stress conditions (tBOOH), both GLUT- and non-GLUT-mediated ^{3}H-DG uptake were decreased. Moreover, the mRNA levels of GLUT1 were quantified and no significant difference under normal or oxidative conditions was found, which means that there is probably no significant alteration in GLUT1 transcription rates.

We also investigated if there could be a more efficient GLUT inhibitor, causing a higher degree of inhibition of ^{3}H-DG uptake, i.e., if the GLUT-mediated component of ^{3}H-DG uptake was underestimated by using cytochalasin B. So, we tested phloretin (2 mM). This compound, at this concentration, was used in a study about transepithelial glucose transport in the same cell line [25]. We could conclude that, although phloretin caused a higher degree of inhibition of ^{3}H-DG uptake (around 80%) than cytochalasin B, it also compromises cell viability (LDH activity assay) and cell proliferation (SRB assay). So, the marked inhibitory effect of phloretin upon ^{3}H-DG uptake is most probably related to the decrease in cell viability and proliferation. Of note, the mentioned study [25] affirms that phloretin (2 mM) completely inhibited transcellular glucose transport, but the effect of this compound on cell integrity was not available. So, taking in consideration the results obtained with phloretin, along with the fact that cytochalasin B was previously used by our group [27], and does not affect cell integrity, cytochalasin B 50 μM appears to be an appropriate inhibitor to define GLUT-mediated transport.

Concerning the second question, we could conclude, by measuring lactate levels in control and tBOOH-treated cultures, that inhibition of ^{3}H-DG uptake by tBOOH did not cause a significant decrease in the amount of lactate produced by the cells.

Two pathways that are activated during oxidative stress stimuli, PI3K/Akt and PKC, were investigated in order to understand if they are involved in the effect of tBOOH upon ^{3}H-DG uptake.

PKC is a serine/threonine-related protein kinase that plays a key role in many cellular functions and affects many signal transduction pathways. There are multiple isoforms of PKC

that function in a wide variety of biological systems. All PKCs contain a C-terminal kinase domain and an N-terminal regulatory domain. Based on primary structure and biochemical characteristics, for instances regulatory domains, these enzymes can be divided into three subfamilies: classical or conventional PKCs (PKC-α, -β1, -β2, and -γ), novel PKCs (PKC-δ, -ε, -θ, and -η) and atypical PKCs (PKC-ζ and -ι/λ), where the first subfamily depends on Ca^{2+} and diacylglycerol (DAG) for activation, the second depends on DAG and the third does not depend of either [79, 80]. Human placental trophoblasts contain at least three PKC isoforms: α, ε and ζ. So, one member from each of the PKC subfamilies can be detected in trophoblasts. [81] Another study showed that PKC β2, δ, ε and ζ were found to be present in both microvillous and basal membranes from term placenta. The -α isoform was observed only on the basal membrane while the -β1 isoform was confined to the microvillous membrane. The basal to microvillous ratios for -β2, -γ, -ε and -ζ ranged between 0.3 and 0.5, demonstrating a substantial asymmetry in plasma membrane localization and immunocytochemistry techniques supported the isoform identification and localization observed in the immunoblotting experiments [82].

When activated, for example at increased levels of glucose, PKC can catalyze the phosphorylation of specific residues of target proteins and thus can alter their activity and consequently cellular metabolism.

In investigations conducted to study this pathway, some inhibitors are used; among them, chelerythrine [83-85].

As for PI3K, it is a lipid heterodimeric kinase that phosphorylates the D-3 position on the inositol ring in phosphoinositides. There are a number of extracellular signals that activate PI3K, such insulin and other growth factors [71]. PI3K/Akt activation promotes glucose metabolism and is dependent on it to inhibit cell death.

PI3K interacts with insulin receptor substrate, phosphorylating it, resulting in the recruitment of the serine-threonine kinase Akt to the plasma membrane. At the membrane, Akt becomes itself phosphorylated. Akt can promote aerobic glycolysis through increased trafficking of GLUT1 to the cell surface, activation of phosphofructokinase and hexokinase activity and stimulation of mTOR [71, 72, 74]. LY294002 is known to be a specific inhibitor of the PI3K/Akt kinase pathway [86, 87].

Using chelerythrine (0.1 μM) as an inhibitor of PKC pathway and LY 294002 (1 μM) as an inhibitor of PI3K/Akt pathway, we could conclude that these pathways are not involved in

the inhibitory effect of tBOOH upon ^{3}H-DG uptake. The PI3K/Akt pathway is described as glucose metabolism-dependent, but in apoptotic conditions [71, 72]. Since oxidative stress imposed by tBOOH was performed under controlled levels, it probably does not constitute an enough cell insult leading to activation of this pathway. In relation to the PKC pathway, it is a pathway described as possibly activated under increased glucose levels [81]. The results presented in this work show a decrease in amount of ^{3}H-DG taken up by the cells, which may be the explanation for the results shown for this pathway.

In the final part of this work, a number of antioxidants were used in order to investigate if they could reverse the effect of tBOOH upon ^{3}H-DG uptake.

First, two inhibitors of endogenous enzymes responsible for ROS formation were studied: apocynin (1 mM), an inhibitor of NADPH-oxidase, and allopurinol (1 mM), an inhibitor of xanthine oxidase. NADPH-oxidase and xanthine-oxidase are two enzymes that, during important metabolic pathways, produce ROS, in particular superoxide. Apocynin has been considered a therapeutic agent in atherosclerotic disease, ozone-induced bronchial hyperresponsiveness, and asthma, among others [88]. Results showed that inhibition of these enzymes did not affect the inhibitory effect of tBOOH upon ^{3}H-DG uptake; so, it can be concluded that the effect of tBOOH is not dependent upon ROS produced by these enzymes in BeWo cells.

The antioxidants α-tocopherol (1 mM) and N-acetylcysteine (NAC) (0.1 mM) were also tested. NAC is an antioxidant that increases intracellular glutathione levels by acting as a precursor in glutathione biosynthesis and as a stimulator of cytosolic enzymes involved in glutathione regeneration [89]. α-tocopherol, as already mentioned in Introduction, is an antioxidant that influences cell membranes' permeability by protecting the latter from free radicals and stabilizing cells in culture [48]. Although the antioxidant capacity of both α-tocopherol and NAC are widely recognized, results regarding these two compounds showed no significant reversive effect upon ^{3}H-DG uptake. This might be due to the fact that the oxidative effect induced by tBOOH overcomes the potential antioxidant effect of these compounds. Moreover, α-tocopherol is a hydrophobic antioxidant and, since the buffer used in all transport experiments had water as the solvent, there is the doubt if the poor solvation of this vitamin might have influenced the results.

Three more antioxidants were tested: resveratrol, quercetin and EGCG ((-) epigallocatechin-3-gallate). These three polyphenols belong to a complex family of phytochemicals that possess several hydroxyl groups on aromatic rings [90].

Table 13: Characteristics regarding resveratrol, quercetin and epigallocatechin-3-gallate.

Molecular structure	Characteristics
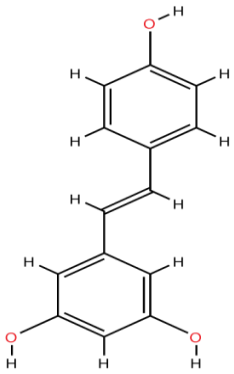	**RESVERATROL** has been proven to be a powerful anti-inflammatory agent, detoxifier of superoxide, cancer chemopreventive, anti-mutagenic and anti-initiative agent, a COX-1 and COX-2 enzymatic inhibitor and a suppressor of PKC- and AP-1 mediated gene expression [91]. It is found in grapes, red wine and mulberries, to name a few [91].
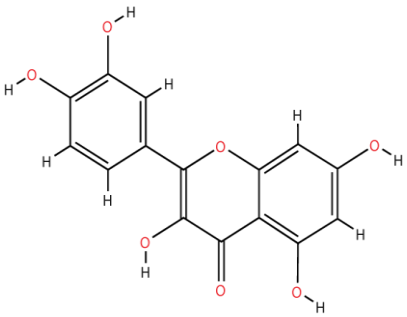	**QUERCETIN** has been proven to chelate iron, which is involved in the hydroxyl radical generation and, along with rutin, seems to have the ability to protect DNA single strand breaks induced by tBOOH, an oxidative stress inducer [35, 92].
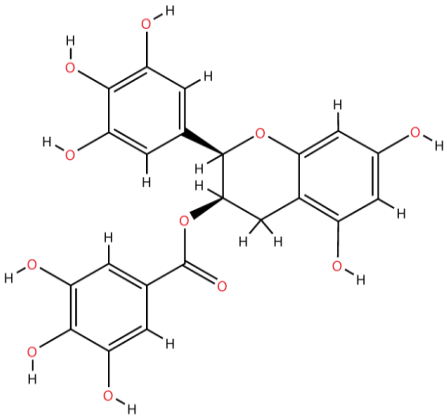	**EPIGALLOCATECHIN-3-GALLATE (EGCG)** is isolated from green tea and has demonstrated chemopreventive and chemotherapeutic actions in cellular and animal models of cancer [93, 94]. EGCG selectively induces apoptosis in human carcinoma cell lines [93, 94]. interferes with angiogenesis [95], inhibits telomerase and DNA methyltransferase [96] and protects cells from lipid peroxidation and DNA damage induced by reactive free radicals [97].

Results regarding these three antioxidants are quite interesting: all three showed a partial reversive effect in relation to the decrease of ^{3}H-DG uptake induced by tBOOH. From the analysis of Table 9, presented in chapter results, we can see that under normal conditions and in the presence of resveratrol, the ^{3}H-DG uptake remains unaffected. Under oxidative stress

conditions, like already discussed above, the total ^{3}H-DG uptake is reduced by more than 30%. However, resveratrol seems to reverse the effect induced by tBOOH in more than 60%. For quercetin (Table 10) and EGCG (Table 11), the results are similar for total uptake, with a reversion of around 50% and 45% of the effect of tBOOH, respectively. Interestingly, the overall analysis shows that the polyphenol reverses completely the effect of tBOOH upon GLUT-mediated uptake.

To answer the last question, one last set of experiments was conducted, in order to investigate if the decrease in apical ^{3}H-DG uptake caused by tBOOH would originate a decrease in the apical-to-basolateral transepithelial transport of ^{3}H-DG. The results showed that, although tBOOH reduced the apical cellular uptake of ^{3}H-DG, it increased the apical-to-basolateral transport of ^{3}H-DG (P_{app}). From these results, several considerations and hypothesis can be considered.

One of the hypotheses proposed is that tight junctions might be compromised in the presence of tBOOH, this affecting (increasing) the paracellular transport of ^{3}H-DG.

Schematizing the hypothesis, the red arrow symbolizes the increase in the passage of ^{3}H-DG across the tight junctions. There have been studies that support this hypothesis, where tBOOH seems to induce the opening of tight junctions [98, 99].

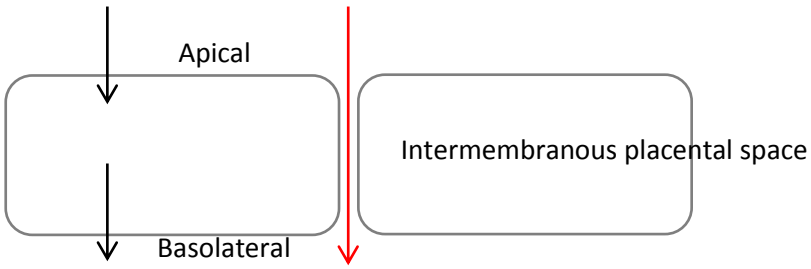

Another hypothesis would be to consider alterations in GLUT transporters' activity at the basolateral membrane, due to tBOOH inhibiting the uptake of basolateral ^{3}H-DG into the cells.

In order to corroborate these hypotheses, more studies should be conducted, so that conclusions about this increase in apical-to-basolateral ^{3}H-DG transport, together with a decrease in the apical uptake, could be taken.

14 Conclusions

The purpose of this study was to find out if the uptake of glucose, the fetus' primary source of energy, would be compromised under oxidative stress conditions. Based in previous studies, tBOOH was chosen as an inducer of oxidative stress in the trophoblastic cell line, BeWo [35, 63, 64]. The proper concentration, tBOOH 100 μM, was chosen after the evaluation of cell integrity and important oxidative stress biomarkers, being the concentration that induced higher oxidative stress levels, without compromising cell integrity.

To evaluate if glucose uptake would be altered under oxidative stress condition, a time-course of ^{3}H-DG uptake was conducted. Results showed that, under normal conditions, 48% of the apical ^{3}H-DG uptake seems to be non-GLUT mediated, leaving 52% of the uptake to GLUT mediation. Under oxidative stress induced by tBOOH 100 μM, the A_{max} of total ^{3}H-DG uptake decreases 33%, through a decrease of 40% of the non-GLUT mediated uptake and of 28% of the GLUT-mediated uptake. However, results of GLUT1 mRNA levels showed no significant alteration under oxidative stress conditions induced by tBOOH, as well as cellular lactate production.

The PKC and the PI3K/Akt pathways were also evaluated under oxidative stress conditions and results showed that these two pathways do not seem to be involved in the inhibitory effect of tBOOH upon ^{3}H-DG uptake.

In the final part of this work, a number of antioxidants were used in order to investigate if they could reverse the effect of oxidative stress upon ^{3}H-DG uptake. Among all antioxidants tested, the polyphenols resveratrol, quercetin and EGCG showed interesting results. With all three, the effect of tBOOH upon ^{3}H-DG uptake was reversed in, at least, 45%, being this increase the result of an increase in GLUT-mediated ^{3}H-DG uptake. This shows that, quite possibly, tBOOH, in the presence of the polyphenol, inhibits the non- GLUT mediated uptake of ^{3}H-DG, while the polyphenol reverses the effect of tBOOH upon GLUT-mediated uptake of ^{3}H-DG.

In relation to the transepithelial ^{3}H-DG transport, results were also very interesting. Although apical cellular uptake of ^{3}H-DG decreased in the presence of tBOOH, the apical-to-basolateral transport of ^{3}H-DG increased in the same conditions. In order to understand these results, more studies are required. So, all findings and conclusions lead to a number of questions:

Would results be any different if another oxidative stress inducer was used? Despite the apparent unaltered mRNA amount, could there be a different GLUT1 protein amount at the membrane and/or a different intrinsic GLUT1 activity? Would higher antioxidants'

concentrations imply a more marked reversive effect of tBOOH? Would results corroborate or contradict the ones found in this project if studies were conducted in another cell line, for instance primary cultures of human trophoblasts, or even *in vivo*?

Considering that many pregnancy pathologies are associated with increased oxidative stress levels, as well as with deregulated glucose levels, the findings in this project shows a relevant first step in order to understand the impact that oxidative stress might have in the uptake of such fundamental fetal nutrient: glucose.

15 References

1. Sarma JV, Ward PA. Oxidants and Redox Signaling in Acute Lung Injury. Wiley. July 2011;1(3).

2. Burton GJ, Jauniaux E. Oxidative stress. Best Pract Res Clin Obstet Gynaecol. 2011 Jun;25(3):287-99. PubMed PMID: 21130690. Pubmed Central PMCID: PMC3101336. eng.

3. Mistry HD, Williams PJ. The importance of antioxidant micronutrients in pregnancy. Oxid Med Cell Longev. 2011;2011:841749. PubMed PMID: 21918714. Pubmed Central PMCID: PMC3171895. eng.

4. Young B, Lowe JS, Stevens A, Heath JW. Wheater's Functional Biology. Ozols I, Whitehouse A, editors. Edimburg: Elsevier Limited; 2006.

5. Kulvietis V, Zalgeviciene V, Didziapetriene J, Rotomskis R. Transport of nanoparticles through the placental barrier. Tohoku J Exp Med. 2011;225(4):225-34. PubMed PMID: 22052087. eng.

6. Prouillac C, Lecoeur S. The role of the placenta in fetal exposure to xenobiotics: importance of membrane transporters and human models for transfer studies. Drug Metab Dispos. 2010 Oct;38(10):1623-35. PubMed PMID: 20606001. eng.

7. Novakovic B, Yuen RK, Gordon L, Penaherrera MS, Sharkey A, Moffett A, et al. Evidence for widespread changes in promoter methylation profile in human placenta in response to increasing gestational age and environmental/stochastic factors. BMC Genomics. 2011;12:529. PubMed PMID: 22032438. Pubmed Central PMCID: PMC3216976. eng.

8. Leach L, Taylor A, Sciota F. Vascular dysfunction in the diabetic placenta: causes and consequences. J Anat. 2009 Jul;215(1):69-76. PubMed PMID: 19563553. Pubmed Central PMCID: PMC2714640. eng.

9. Ni Z, Mao Q. ATP-binding cassette efflux transporters in human placenta. Curr Pharm Biotechnol. 2011 Apr;12(4):674-85. PubMed PMID: 21118087. Pubmed Central PMCID: PMC3081393. eng.

10. Sastry BV. Techniques to study human placental transport. Adv Drug Deliv Rev. 1999 Jun;38(1):17-39. PubMed PMID: 10837744. ENG.

11. van der Aa EM, Peereboom-Stegeman JH, Noordhoek J, Gribnau FW, Russel FG. Mechanisms of drug transfer across the human placenta. Pharm World Sci. 1998 Aug;20(4):139-48. PubMed PMID: 9762726. eng.

12. Sibley C, Glazier J, D'Souza S. Placental transporter activity and expression in relation to fetal growth. Exp Physiol. 1997 Mar;82(2):389-402. PubMed PMID: 9129953. eng.

13. M CB. Human Embriology and Developmental Biology 4th Edition: Mosby; 2008. 560 p.

14. Schneider H, Reiber W, Sager R, Malek A. Asymmetrical transport of glucose across the in vitro perfused human placenta. Placenta. 2003 Jan;24(1):27-33. PubMed PMID: 12495656. eng.

15. Hay WW. Placental-fetal glucose exchange and fetal glucose metabolism. Trans Am Clin Climatol Assoc. 2006;117:321-39; discussion 39-40. PubMed PMID: 18528484. Pubmed Central PMCID: PMC1500912. eng.

16. Baumann MU, Deborde S, Illsley NP. Placental glucose transfer and fetal growth. Endocrine. 2002 Oct;19(1):13-22. PubMed PMID: 12583599. eng.

17. Barta E, Drugan A. Glucose transport from mother to fetus--a theoretical study. J Theor Biol. 2010 Apr;263(3):295-302. PubMed PMID: 20006624. eng.

18. Gaither K, Quraishi AN, Illsley NP. Diabetes alters the expression and activity of the human placental GLUT1 glucose transporter. J Clin Endocrinol Metab. 1999 Feb;84(2):695-701. PubMed PMID: 10022440. eng.

19. Carruthers A, DeZutter J, Ganguly A, Devaskar SU. Will the original glucose transporter isoform please stand up! Am J Physiol Endocrinol Metab. 2009 Oct;297(4):E836-48. PubMed PMID: 19690067. Pubmed Central PMCID: PMC2763785. eng.

20. Liu F, Soares MJ, Audus KL. Permeability properties of monolayers of the human trophoblast cell line BeWo. Am J Physiol. 1997 Nov;273(5 Pt 1):C1596-604. PubMed PMID: 9374645. eng.

21. Joost HG, Thorens B. The extended GLUT-family of sugar/polyol transport facilitators: nomenclature, sequence characteristics, and potential function of its novel members (review). Mol Membr Biol. 2001 2001 Oct-Dec;18(4):247-56. PubMed PMID: 11780753. eng.

22. Illsley NP. Glucose transporters in the human placenta. Placenta. 2000 Jan;21(1):14-22. PubMed PMID: 10692246. eng.

23. von Wolff M, Ursel S, Hahn U, Steldinger R, Strowitzki T. Glucose transporter proteins (GLUT) in human endometrium: expression, regulation, and function throughout the menstrual cycle and in early pregnancy. J Clin Endocrinol Metab. 2003 Aug;88(8):3885-92. PubMed PMID: 12915684. eng.

24. Baumann MU, Zamudio S, Illsley NP. Hypoxic upregulation of glucose transporters in BeWo choriocarcinoma cells is mediated by hypoxia-inducible factor-1. Am J Physiol Cell Physiol. 2007 Jul;293(1):C477-85. PubMed PMID: 17442736. eng.

25. Vardhana PA, Illsley NP. Transepithelial glucose transport and metabolism in BeWo choriocarcinoma cells. Placenta. 2002 2002 Sep-Oct;23(8-9):653-60. PubMed PMID: 12361684. eng.

26. Shah SW, Zhao H, Low SY, Mcardle HJ, Hundal HS. Characterization of glucose transport and glucose transporters in the human choriocarcinoma cell line, BeWo. Placenta. 1999 Nov;20(8):651-9. PubMed PMID: 10527819. eng.

27. Araújo JR, Gonçalves P, Martel F. Modulation of glucose uptake in a human choriocarcinoma cell line (BeWo) by dietary bioactive compounds and drugs of abuse. J Biochem. 2008 Aug;144(2):177-86. PubMed PMID: 18424810. eng.

28. Gude NM, Stevenson JL, Murthi P, Rogers S, Best JD, Kalionis B, et al. Expression of GLUT12 in the fetal membranes of the human placenta. Placenta. 2005 Jan;26(1):67-72. PubMed PMID: 15664413. eng.

29. Brown K, Heller DS, Zamudio S, Illsley NP. Glucose transporter 3 (GLUT3) protein expression in human placenta across gestation. Placenta. 2011 Dec;32(12):1041-9. PubMed PMID: 22000473. Pubmed Central PMCID: PMC3272879. eng.

30. Bibee KP, Illsley NP, Moley KH. Asymmetric syncytial expression of GLUT9 splice variants in human term placenta and alterations in diabetic pregnancies. Reprod Sci. 2011 Jan;18(1):20-7. PubMed PMID: 20926839. Pubmed Central PMCID: PMC3343070. eng.

31. Halliwell B. Oxidative stress in cell culture: an under-appreciated problem? FEBS Lett. 2003 Apr;540(1-3):3-6. PubMed PMID: 12681474. eng.

32. Dröge W. Free radicals in the physiological control of cell function. Physiol Rev. 2002 Jan;82(1):47-95. PubMed PMID: 11773609. eng.

33. Dalle-Donne I, Rossi R, Colombo R, Giustarini D, Milzani A. Biomarkers of oxidative damage in human disease. Clin Chem. 2006 Apr;52(4):601-23. PubMed PMID: 16484333. eng.

34. Dalle-Donne I, Rossi R, Giustarini D, Milzani A, Colombo R. Protein carbonyl groups as biomarkers of oxidative stress. Clin Chim Acta. 2003 Mar;329(1-2):23-38. PubMed PMID: 12589963. eng.

35. Aherne SA, O'Brien NM. Mechanism of protection by the flavonoids, quercetin and rutin, against tert-butylhydroperoxide- and menadione-induced DNA single strand breaks in Caco-2 cells. Free Radic Biol Med. 2000 Sep;29(6):507-14. PubMed PMID: 11025194. eng.

36. Silva E, Soares-da-Silva P. Reactive oxygen species and the regulation of renal Na+-K+-ATPase in opossum kidney cells. Am J Physiol Regul Integr Comp Physiol. 2007 Oct;293(4):R1764-70. PubMed PMID: 17670864. eng.

37. Mitjavila MT, Moreno JJ. The effects of polyphenols on oxidative stress and the arachidonic acid cascade. Implications for the prevention/treatment of high prevalence diseases. Biochem Pharmacol. 2012 Jul. PubMed PMID: 22858365. ENG.

38. Valko M, Leibfritz D, Moncol J, Cronin MT, Mazur M, Telser J. Free radicals and antioxidants in normal physiological functions and human disease. Int J Biochem Cell Biol. 2007;39(1):44-84. PubMed PMID: 16978905. eng.

39. Poli G, Leonarduzzi G, Biasi F, Chiarpotto E. Oxidative stress and cell signalling. Curr Med Chem. 2004 May;11(9):1163-82. PubMed PMID: 15134513. eng.

40. Burton GJ, Yung HW, Cindrova-Davies T, Charnock-Jones DS. Placental endoplasmic reticulum stress and oxidative stress in the pathophysiology of unexplained intrauterine growth restriction and early onset preeclampsia. Placenta. 2009 Mar;30 Suppl A:S43-8. PubMed PMID: 19081132. Pubmed Central PMCID: PMC2684656. eng.

41. Tuuli MG, Longtine MS, Nelson DM. Review: Oxygen and trophoblast biology--a source of controversy. Placenta. 2011 Mar;32 Suppl 2:S109-18. PubMed PMID: 21216006. eng.

42. Burton GJ, Jauniaux E, Charnock-Jones DS. The influence of the intrauterine environment on human placental development. Int J Dev Biol. 2010;54(2-3):303-12. PubMed PMID: 19757391. eng.

43. Myatt L. Review: Reactive oxygen and nitrogen species and functional adaptation of the placenta. Placenta. 2010 Mar;31 Suppl:S66-9. PubMed PMID: 20110125. Pubmed Central PMCID: PMC2832707. eng.

44. Hu R, Jin H, Zhou S, Yang P, Li X. Proteomic analysis of hypoxia-induced responses in the syncytialization of human placental cell line BeWo. Placenta. 2007 2007 May-Jun;28(5-6):399-407. PubMed PMID: 17098281. eng.

45. Valko M, Rhodes CJ, Moncol J, Izakovic M, Mazur M. Free radicals, metals and antioxidants in oxidative stress-induced cancer. Chem Biol Interact. 2006 Mar;160(1):1-40. PubMed PMID: 16430879. eng.

46. Singh BK, Tripathi M, Pandey PK, Kakkar P. Alteration in mitochondrial thiol enhances calcium ion dependent membrane permeability transition and dysfunction in vitro: a cross-talk between mtThiol, Ca(2+), and ROS. Mol Cell Biochem. 2011 Nov;357(1-2):373-85. PubMed PMID: 21748338. eng.

47. Poston L, Raijmakers MT. Trophoblast oxidative stress, antioxidants and pregnancy outcome--a review. Placenta. 2004 Apr;25 Suppl A:S72-8. PubMed PMID: 15033311. eng.

48. Urban K, Höhling HJ, Lüttenberg B, Szuwart T, Plate U. An in vitro study of osteoblast vitality influenced by the vitamins C and E. Head Face Med. 2012 Sep;8(1):25. PubMed PMID: 23021517. ENG.

49. Martel F, Monteiro R, Calhau C. Effect of polyphenols on the intestinal and placental transport of some bioactive compounds. Nutr Res Rev. 2010 Jun;23(1):47-64. PubMed PMID: 20392307. eng.

50. Manna C, D'Angelo S, Migliardi V, Loffredi E, Mazzoni O, Morrica P, et al. Protective effect of the phenolic fraction from virgin olive oils against oxidative stress in human cells. J Agric Food Chem. 2002 Oct;50(22):6521-6. PubMed PMID: 12381144. eng.

51. Bravo L. Polyphenols: chemistry, dietary sources, metabolism, and nutritional significance. Nutr Rev. 1998 Nov;56(11):317-33. PubMed PMID: 9838798. eng.

52. Jovanovic L. Nutrition and pregnancy: the link between dietary intake and diabetes. Curr Diab Rep. 2004 Aug;4(4):266-72. PubMed PMID: 15265469. eng.

53. Cameron N, Demerath EW. Critical periods in human growth and their relationship to diseases of aging. Am J Phys Anthropol. 2002;Suppl 35:159-84. PubMed PMID: 12653312. eng.

54. Leduc L, Levy E, Bouity-Voubou M, Delvin E. Fetal programming of atherosclerosis: possible role of the mitochondria. Eur J Obstet Gynecol Reprod Biol. 2010 Apr;149(2):127-30. PubMed PMID: 20053495. eng.

55. Tzanetakou IP, Mikhailidis DP, Perrea DN. Nutrition During Pregnancy and the Effect of Carbohydrates on the Offspring's Metabolic Profile: In Search of the "Perfect Maternal Diet". Open Cardiovasc Med J. 2011;5:103-9. PubMed PMID: 21673843. Pubmed Central PMCID: PMC3111740. eng.

56. Keating E, Lemos C, Gonçalves P, Martel F. Acute and chronic effects of some dietary bioactive compounds on folic acid uptake and on the expression of folic acid transporters by the

human trophoblast cell line BeWo. J Nutr Biochem. 2008 Feb;19(2):91-100. PubMed PMID: 17531458. eng.

57. Theuerkauf RS, Ahammer H, Siwetz M, Helige C, Dohr G, Walcher W, et al. Measurement of cell death by oxidative stress in three-dimensional spheroids from trophoblast and in fragments of decidua tissue. J Reprod Immunol. 2010 May;85(1):63-70. PubMed PMID: 20227766. eng.

58. Shibata M, Hakuno F, Yamanaka D, Okajima H, Fukushima T, Hasegawa T, et al. Paraquat-induced oxidative stress represses phosphatidylinositol 3-kinase activities leading to impaired glucose uptake in 3T3-L1 adipocytes. J Biol Chem. 2010 Jul;285(27):20915-25. PubMed PMID: 20430890. Pubmed Central PMCID: PMC2898352. eng.

59. Hempstock J, Jauniaux E, Greenwold N, Burton GJ. The contribution of placental oxidative stress to early pregnancy failure. Hum Pathol. 2003 Dec;34(12):1265-75. PubMed PMID: 14691912. eng.

60. Orendi K, Kivity V, Sammar M, Grimpel Y, Gonen R, Meiri H, et al. Placental and trophoblastic in vitro models to study preventive and therapeutic agents for preeclampsia. Placenta. 2011 Feb;32 Suppl:S49-54. PubMed PMID: 21257083. eng.

61. Keating E, Lemos C, Azevedo I, Martel F. Characteristics of thiamine uptake by the BeWo human trophoblast cell line. J Biochem Mol Biol. 2006 Jul;39(4):383-93. PubMed PMID: 16889681. eng.

62. Orendi K, Gauster M, Moser G, Meiri H, Huppertz B. The choriocarcinoma cell line BeWo: syncytial fusion and expression of syncytium-specific proteins. Reproduction. 2010 Nov;140(5):759-66. PubMed PMID: 20696850. eng.

63. Garcia-Cohen EC, Marin J, Diez-Picazo LD, Baena AB, Salaices M, Rodriguez-Martinez MA. Oxidative stress induced by tert-butyl hydroperoxide causes vasoconstriction in the aorta from hypertensive and aged rats: role of cyclooxygenase-2 isoform. J Pharmacol Exp Ther. 2000 Apr;293(1):75-81. PubMed PMID: 10734155. eng.

64. Fernandes R, Hosoya K, Pereira P. Reactive oxygen species downregulate glucose transport system in retinal endothelial cells. Am J Physiol Cell Physiol. 2011 Apr;300(4):C927-36. PubMed PMID: 21228321. eng.

65. Gonçalves P, Araújo JR, Pinho MJ, Martel F. In vitro studies on the inhibition of colon cancer by butyrate and polyphenolic compounds. Nutr Cancer. 2011;63(2):282-94. PubMed PMID: 21207318. eng.

66. Gonçalves P, Gregório I, Martel F. The short-chain fatty acid butyrate is a substrate of breast cancer resistance protein. Am J Physiol Cell Physiol. 2011 Nov;301(5):C984-94. PubMed PMID: 21775706. eng.

67. Capela JP, Macedo C, Branco PS, Ferreira LM, Lobo AM, Fernandes E, et al. Neurotoxicity mechanisms of thioether ecstasy metabolites. Neuroscience. 2007 Jun;146(4):1743-57. PubMed PMID: 17467183. eng.

68. Bradford MM. A rapid and sensitive method for the quantitation of microgram quantities of protein utilizing the principle of protein-dye binding. Anal Biochem. 1976 May;72:248-54. PubMed PMID: 942051. eng.

69. Muzyka A, Tarkany O, Yelizanov V, Sergienko U, Boichuk A. GraphPad Prism (version 4.03) for Windows. San Diego, USA2005.

70. Talior I, Yarkoni M, Bashan N, Eldar-Finkelman H. Increased glucose uptake promotes oxidative stress and PKC-delta activation in adipocytes of obese, insulin-resistant mice. Am J Physiol Endocrinol Metab. 2003 Aug;285(2):E295-302. PubMed PMID: 12857675. eng.

71. Riley JK, Carayannopoulos MO, Wyman AH, Chi M, Moley KH. Phosphatidylinositol 3-kinase activity is critical for glucose metabolism and embryo survival in murine blastocysts. J Biol Chem. 2006 Mar;281(9):6010-9. PubMed PMID: 16272157. eng.

72. Coloff JL, Mason EF, Altman BJ, Gerriets VA, Liu T, Nichols AN, et al. Akt requires glucose metabolism to suppress puma expression and prevent apoptosis of leukemic T cells. J Biol Chem. 2011 Feb;286(7):5921-33. PubMed PMID: 21159778. Pubmed Central PMCID: PMC3037705. eng.

73. Go YM, Jones DP. Redox control systems in the nucleus: mechanisms and functions. Antioxid Redox Signal. 2010 Aug;13(4):489-509. PubMed PMID: 20210649. Pubmed Central PMCID: PMC2935340. eng.

74. Mieyal JJ, Gallogly MM, Qanungo S, Sabens EA, Shelton MD. Molecular mechanisms and clinical implications of reversible protein S-glutathionylation. Antioxid Redox Signal. 2008 Nov;10(11):1941-88. PubMed PMID: 18774901. Pubmed Central PMCID: PMC2774718. eng.

75. Fernandes ER, Carvalho FD, Remião FG, Bastos ML, Pinto MM, Gottlieb OR. Hepatoprotective activity of xanthones and xanthonolignoids against tert-butylhydroperoxide-induced toxicity in isolated rat hepatocytes--comparison with silybin. Pharm Res. 1995 Nov;12(11):1756-60. PubMed PMID: 8592682. eng.

76. Radak Z, Zhao Z, Goto S, Koltai E. Age-associated neurodegeneration and oxidative damage to lipids, proteins and DNA. Mol Aspects Med. 2011 Aug;32(4-6):305-15. PubMed PMID: 22020115. eng.

77. Hagfors L, Leanderson P, Sköldstam L, Andersson J, Johansson G. Antioxidant intake, plasma antioxidants and oxidative stress in a randomized, controlled, parallel, Mediterranean dietary intervention study on patients with rheumatoid arthritis. Nutr J. 2003 Jul;2:5. PubMed PMID: 12952549. Pubmed Central PMCID: PMC194256. eng.

78. Wright EM, Martín MG, Turk E. Intestinal absorption in health and disease--sugars. Best Pract Res Clin Gastroenterol. 2003 Dec;17(6):943-56. PubMed PMID: 14642859. eng.

79. Corbalán-García S, Gómez-Fernández JC. Protein kinase C regulatory domains: the art of decoding many different signals in membranes. Biochim Biophys Acta. 2006 Jul;1761(7):633-54. PubMed PMID: 16809062. eng.

80. Konishi H, Tanaka M, Takemura Y, Matsuzaki H, Ono Y, Kikkawa U, et al. Activation of protein kinase C by tyrosine phosphorylation in response to H2O2. Proc Natl Acad Sci U S A. 1997 Oct;94(21):11233-7. PubMed PMID: 9326592. Pubmed Central PMCID: PMC23425. eng.

81. Karl PI, Divald A. Protein kinase C in cultured human placental trophoblasts: identification of isoforms and role in cAMP signalling. Biochem J. 1996 Dec;320 (Pt 3):831-6. PubMed PMID: 9003369. Pubmed Central PMCID: PMC1218004. eng.

82. Ruzycky AL, Jansson T, Illsley NP. Differential expression of protein kinase C isoforms in the human placenta. Placenta. 1996 Sep;17(7):461-9. PubMed PMID: 8899875. eng.

83. Simonis G, Wiedemann S, Schwarz K, Christ T, Sedding DG, Yu X, et al. Chelerythrine treatment influences the balance of pro- and anti-apoptotic signaling pathways in the remote myocardium after infarction. Mol Cell Biochem. 2008 Mar;310(1-2):119-28. PubMed PMID: 18060473. eng.

84. Harmati G, Papp F, Szentandrássy N, Bárándi L, Ruzsnavszky F, Horváth B, et al. Effects of the PKC inhibitors chelerythrine and bisindolylmaleimide I (GF 109203X) on delayed rectifier K+ currents. Naunyn Schmiedebergs Arch Pharmacol. 2011 Feb;383(2):141-8. PubMed PMID: 21120453. eng.

85. Herbert JM, Augereau JM, Gleye J, Maffrand JP. Chelerythrine is a potent and specific inhibitor of protein kinase C. Biochem Biophys Res Commun. 1990 Nov;172(3):993-9. PubMed PMID: 2244923. eng.

86. Barancík M, Bohácová V, Sedlák J, Sulová Z, Breier A. LY294,002, a specific inhibitor of PI3K/Akt kinase pathway, antagonizes P-glycoprotein-mediated multidrug resistance. Eur J Pharm Sci. 2006 Dec;29(5):426-34. PubMed PMID: 17010577. eng.

87. Sheth P, Basuroy S, Li C, Naren AP, Rao RK. Role of phosphatidylinositol 3-kinase in oxidative stress-induced disruption of tight junctions. J Biol Chem. 2003 Dec;278(49):49239-45. PubMed PMID: 14500730. eng.

88. Stefanska J, Pawliczak R. Apocynin: molecular aptitudes. Mediators Inflamm. 2008;2008:106507. PubMed PMID: 19096513. Pubmed Central PMCID: PMC2593395. eng.

89. Chandramani Shivalingappa P, Jin H, Anantharam V, Kanthasamy A. N-Acetyl Cysteine Protects against Methamphetamine-Induced Dopaminergic Neurodegeneration via Modulation of Redox Status and Autophagy in Dopaminergic Cells. Parkinsons Dis. 2012;2012:424285. PubMed PMID: 23056996. Pubmed Central PMCID: PMC3465903. eng.

90. Tsao R. Chemistry and biochemistry of dietary polyphenols. Nutrients. 2010 Dec;2(12):1231-46. PubMed PMID: 22254006. Pubmed Central PMCID: PMC3257627. eng.

91. Leonard SS, Xia C, Jiang BH, Stinefelt B, Klandorf H, Harris GK, et al. Resveratrol scavenges reactive oxygen species and effects radical-induced cellular responses. Biochem Biophys Res Commun. 2003 Oct;309(4):1017-26. PubMed PMID: 13679076. eng.

92. Ferrali M, Signorini C, Caciotti B, Sugherini L, Ciccoli L, Giachetti D, et al. Protection against oxidative damage of erythrocyte membrane by the flavonoid quercetin and its relation to iron chelating activity. FEBS Lett. 1997 Oct;416(2):123-9. PubMed PMID: 9369196. eng.

93. Lambert JD, Yang CS. Mechanisms of cancer prevention by tea constituents. J Nutr. 2003 Oct;133(10):3262S-7S. PubMed PMID: 14519824. eng.

94. Borska S, Gebarowska E, Wysocka T, Drag-Zalesińska M, Zabel M. Induction of apoptosis by EGCG in selected tumour cell lines in vitro. Folia Histochem Cytobiol. 2003;41(4):229-32. PubMed PMID: 14677763. eng.

95. Lee YK, Bone ND, Strege AK, Shanafelt TD, Jelinek DF, Kay NE. VEGF receptor phosphorylation status and apoptosis is modulated by a green tea component, epigallocatechin-3-gallate (EGCG), in B-cell chronic lymphocytic leukemia. Blood. 2004 Aug;104(3):788-94. PubMed PMID: 14996703. eng.

96. Yokoyama M, Noguchi M, Nakao Y, Pater A, Iwasaka T. The tea polyphenol, (-)-epigallocatechin gallate effects on growth, apoptosis, and telomerase activity in cervical cell lines. Gynecol Oncol. 2004 Jan;92(1):197-204. PubMed PMID: 14751158. eng.

97. Saffari Y, Sadrzadeh SM. Green tea metabolite EGCG protects membranes against oxidative damage in vitro. Life Sci. 2004 Feb;74(12):1513-8. PubMed PMID: 14729400. eng.

98. Nagira M, Tomita M, Mizuno S, Kumata M, Ayabe T, Hayashi M. Ischemia/reperfusion injury in the monolayers of human intestinal epithelial cell line caco-2 and its recovery by antioxidants. Drug Metab Pharmacokinet. 2006 Jun;21(3):230-7. PubMed PMID: 16858127. eng.

99. Kim HJ, Lee EK, Park MH, Ha YM, Jung KJ, Kim MS, et al. Ferulate Protects the Epithelial Barrier by Maintaining Tight Junction Protein Expression and Preventing Apoptosis in Tert-Butyl Hydroperoxide-Induced Caco-2 Cells. Phytother Res. 2012 May. PubMed PMID: 22610911. ENG.